IOP Publishing Journal of Neural Engineering

A Scoping Review of Current and Emerging Techniques for Evaluation of Peripheral Nerve Health, Degeneration and Regeneration: Part 2, Non-Invasive Imaging

Ross Mandeville, MD[1], Swati Deshmukh, MD[2], Ek Tsoon Tan, PhD[3], Viksit Kumar, PhD[4], Benjamin Sanchez, PhD[5], Arriyan Dowlatshahi, MD[6], Justin Luk[7], Reiner See, MD[8], Carl Leochico, MD[9], Jas Thum, MD[7], Stanley Bazarek, MD, PhD[10], Benjamin Johnston, MD, PhD [10], Justin Brown, MD[7], Jim Wu, MD[2], Darryl Sneag, MD[3], Seward Rutkove, MD[1]

[1] Department of Neurology, Beth Israel Deaconess Medical Center, Boston, MA 02215 USA
[2] Department of Radiology, Beth Israel Deaconess Medical Center, Boston, MA 02215 USA
[3] Department of Radiology, Hospital for Special Surgery, New York, NY 10021 USA
[4] Department of Radiology, Massachusetts General Hospital, Boston MA 02114 USA
[5] Department Electrical and Computer Engineering, University of Utah, Salt Lake City, UT 84112 USA
[6] Department of Surgery, Beth Israel Deaconess Medical Center, Boston, MA 02215 USA
[7] Department of Neurosurgery, Massachusetts General Hospital, Boston MA 02114 USA
[8] Department of Neurology, Massachusetts General Hospital, Boston MA 02114 USA
[9] Department of Physical Medicine and Rehabilitation, St. Luke's Medical Center, Global City, Taguig, Philippines
[10]Department of Neurosurgery, Brigham and Women's Hospital, Boston MA 02115 USA

E-mail: rmandevi@bidmc.harvard.edu

Abstract

Peripheral neuroregenerative research and therapeutic options are expanding exponentially. With this expansion comes an increasing need to reliably evaluate and quantify nerve health. Valid and responsive measures of the nerve status are essential for both clinical and research purposes for diagnosis, longitudinal follow-up, and monitoring the impact of any intervention. Furthermore, novel biomarkers can elucidate regenerative mechanisms and open new avenues for research. Without such measures, clinical decision-making is impaired, and research becomes more costly, time-consuming, and sometimes infeasible. Part 1 of this two-part scoping review focused on neurophysiology. In Part 2, we identify and critically examine many current and emerging non-invasive imaging techniques that have the potential to evaluate peripheral nerve health, particularly from the perspective of regenerative therapies and research.

Keywords: Nerve regeneration, Peripheral nerve imaging, Muscle imaging, Quantitative, MR Neurography, Neuromuscular Ultrasound

Introduction

Peripheral nerves are vital to how we perceive and interact with our environment and each other; even mild injury can lead to life-changing consequences[1–3]. Without the protection of bone, and often being very superficial and vulnerable, peripheral nerves are frequently damaged in diverse ways, both traumatically and spontaneously[4,5]. The combination of their importance and the prevalence of injury makes the management of peripheral nerve pathology one of the greatest challenges to our society. Fortunately, rapid expansion is occurring in therapies designed to promote peripheral reinnervation or slow degeneration across a multitude of conditions[6–10]. However, without accurate quantification and characterization of nerve health, clinical decision-making, translation of neurorestorative therapies, and indeed generation of new therapeutic lines of research are slowed by an order of magnitude. Generally, peripheral nerve evaluation continues to rely heavily on clinical examination and standard neurophysiology, especially in the clinical domain. These standard investigations attempt to classify by spatial distribution, presence of demyelination or axon loss, and severity to inform the pathological process and guide management. In animal research, invasive histological markers, basic neurophysiology, and behavior tend to be most employed. The capacity to quantify axonal integrity or detect degenerating and regenerating nerve fibers, essential for evaluating nerve health and regeneration, is rarely evaluated from a non-invasive imaging perspective.

This scoping review represents Part 2 of a two-part review on current and emerging techniques in the evaluation of nerve health. In Part 1, we performed a scoping review of the same subject but focused on neurophysiological techniques[11] (in submission). In Part 2, the objective is firstly to cast a wide net to systematically identify and collate non-invasive imaging techniques that can, or have a reasonable potential to, evaluate peripheral nerve health, including approaches and techniques that may have not previously been applied to peripheral nerve. Our second objective is to provide commentary on their value, practicality, and future direction from a cross-specialty perspective. The goal is to provide a broad foundation from where effective clinical and research design decisions can be tailored, as well as to highlight and encourage areas of basic and translational science that may prove fruitful in advancing peripheral nerve imaging. The scope of the review is limited to non-invasive or intraoperative techniques. This is in part due to the burgeoning literature and advances in more invasive imaging techniques and microscopy that bridge across the fields of histology and imaging. The boundaries are not clear-cut, and subjective decisions have been made as to which techniques fall within the scope of this review, with magnetic resonance, ultrasound, and photoacoustic based imaging techniques representing its backbone.

Nerve health can be quantified in many ways that can be categorized grossly into structure and function. While many excellent reviews exist that are concerned with assessing varied polyneuropathies and entrapment neuropathies using extraneural gross morphology, including demyelinating conditions, this review predominantly focuses on imaging the state of innervation and histological structure pertinent to degeneration and regeneration, regardless of the pathological mechanisms of injury. Beyond quantifying the axonal quality and number, even a nerve devoid of axons has a level of health associated with it that is vital to understand clinically and in research; the nerve may be so degenerated as to not accept new axons, or it may be primed by Wallerian degeneration to spur axonal regeneration, and differentiating such characteristics is essential for optimizing outcomes.

While a formal systematic review is not possible when hypothesis generation is the goal, a scoping review methodology[12] was applied to ensure wide coverage of potential techniques, including techniques that may have yet to be applied to peripheral nerve. We briefly review the more common current approaches to imaging peripheral nerves before focusing on selected promising and emerging techniques that were identified with the aid of the structured scoping searches in combination with discussion among authors selected for their variety of specialties and experience.

The companion scoping review of the same subject but focused on neurophysiology (under review) assesses nerve functionality, complementing the more structurally oriented measures discussed within this review. However, imaging and neurophysiology are not the only methods of assessing nerve; it should be emphasized when deciding on research design or clinical management, the entire range of nerve evaluation approaches need to be considered including, histological and lab-based assays, clinical exam, patient reported outcomes, survival, and behavior[13]. Next, we discussed methodology of the review and the results prior to discussing the imaging techniques from the perspective of validity, practicality, and future direction.

Methods

The same methodology was applied as that of the companion review focused on neurophysiology (under review). The scoping review involved a search of PubMed, Embase, Web of Science, and Google Scholar[12] to answer the question “what imaging techniques currently assess peripheral nerve health in clinical and research practice, and what are the techniques that show promise?”. Using PRISMA-ScR[14,15] guidelines and aid from our institutions librarians, we developed a comprehensive search strategy to identify published and gray literature sources. Briefly, the initial limited search using title, abstract and associated index terms in PubMed, along with iterative discussion among authors and colleagues, curated the list of terms for inclusion of current and potential techniques. The second search applied these terms across all 4 databases, which included a Google Scholar search through screening of the first 400 records. Search results were augmented by review of the references of selected articles, as well as review of thoughts on future directions that may indicate additional potential or emerging techniques. We did not apply restrictions on language, dates, or article type. Imaging search terms (such as MR neurography, ultrasound, photoacoustic) were connected via “AND” Boolean statements to nerve health statements (such as injury, regeneration, denervation, neuropathy). “NOT” statements (referring to unrelated disorders and anatomy) were used to refine result numbers, and these were collected during the initial limited PubMed search.

Any technology that had the potential to image nerve non-invasively or intraoperatively was initially deemed eligible for further consideration. This included imaging techniques that allowed monitoring over time and at a depth of at least several millimeters. Given the absence of a clearly demarcated line dividing invasive and non-invasive imaging techniques, as well as time and resource constraints, those techniques on the border of inclusion were identified and separately discussed as to appropriateness of inclusion or not amongst the study authors. Of note, most microscopy techniques were considered out of scope due to being generally limited to sub-millimeter depths and usually requiring more invasive methods. Some methods overlapped with the scoping review focused on neurophysiology; most notably, electrical impedance tomography (EIT), which is an imaging modality but included in the neurophysiology review due to its provenance and significant component of neurophysiology. Additionally, imaging technologies that could be used to stimulate a nerve action potential were

included in the review focused on neurophysiology including, ultrasound, magnetic resonance, and optical stimulation. We included evaluation of muscle as a surrogate for nerve health because it is so closely related with motor axons and nerve health. Sources referring to standard imaging were excluded but discussed while referencing established textbooks and seminal articles; however, if the source described a novel implementation of standard techniques, this was included. After iterative discussion amongst the authors, articles were selected based on their contribution in terms of performance characteristics, practicality, and underlying mechanisms and suggestions for future advances. Final searches were completed in March 2023 and processed using Covidence and Zotero software. Although, a degree of subjectivity was unavoidable, bias was minimized by using broad and a priori search protocols, as well as the involvement of cross-disciplinary authors.

Results

The results of the scoping search are detailed below in the flow diagram (Fig 1). The search of the 4 databases returned 2711 texts. Titles and abstracts of all texts were reviewed by the authors, as well as the references of those selected as most informative about performance characteristics and mechanisms. This resulted in 533 texts deemed relevant for the relationship between imaging and nerve health, and full texts were downloaded. Authors discussed and critically evaluated the articles, selecting those most relevant to performance characteristics, mechanisms, and potential as a measure of nerve health to be included for discussion and referencing in the review (265 texts).

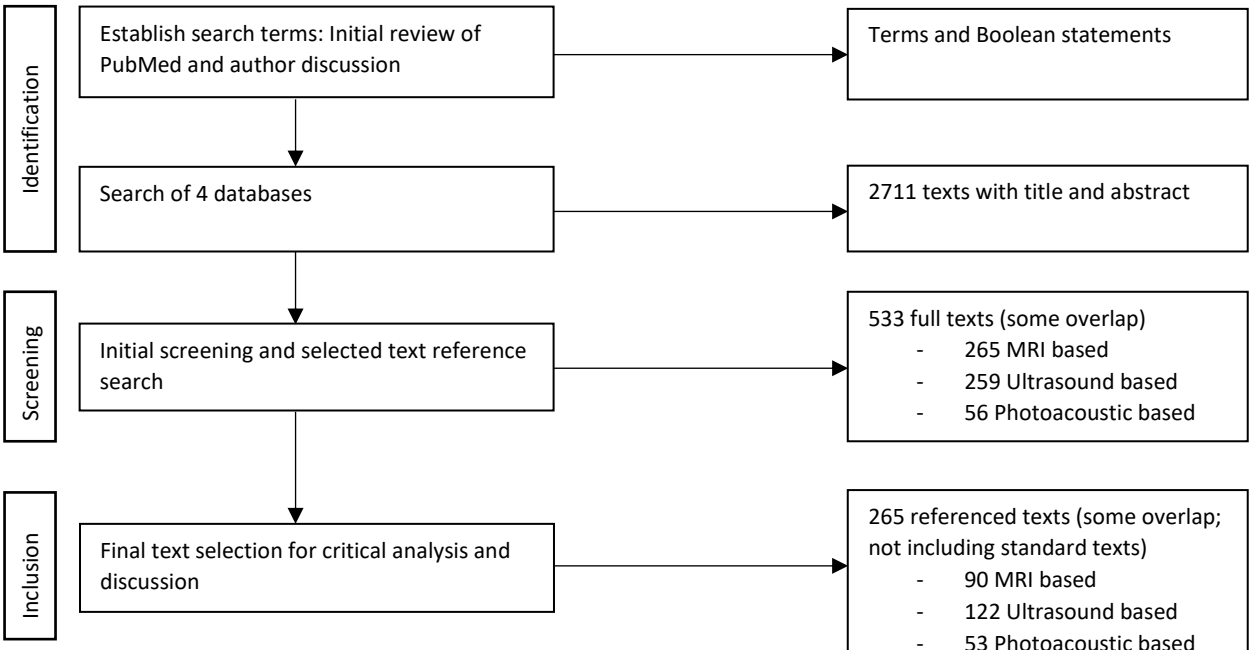

Figure 1: Search Flow Chart. MRI: Magnetic Resonance Imaging.

1. MAGNETIC RESONANCE IMAGING TECHNIQUES

1.1 Neuromuscular MRI

MRI has long evaluated gross extraneural peripheral nerve structural abnormalities such as nerve continuity and intra- or extraneural masses[16]. However, advances in spatial resolution and processing, as well as more availability of clinical MRI with higher magnetic field strengths (3 or 7 Tesla), now make

MRI increasingly suitable for evaluating internal fascicular architecture[17–22]. Secondary signal alterations in denervated muscle offers further insight into nerve health in a conceptually similar manner to studying muscle neurophysiology with electromyography (EMG)[23,24], and interest in muscle quantification is growing as the realization of its diagnostic utility is becoming clearer.

MR technology continues to advance rapidly in the assessment of both nerve and muscle. An array of current and emerging quantitative MR approaches to neuromuscular evaluation are briefly reviewed below.

1.1.1 MR Neurography

The term 'MR neurography' (MRN), coined in the early 1990s, refers to the application of specific MR pulse sequences to improve peripheral nerve visualization [25–27]. Generally, fascicular bundles are isointense to slightly hyperintense to muscle on T2-weighted pulse sequences[21]. Fat suppression is important to increase contrast between nerves and adjacent soft tissues, mainly muscle. Vascular suppression techniques may also be useful to suppress slow-flowing vessels that can confound reliable identification of adjacent peripheral nerves[17]. Administering intravenous gadolinium contrast is useful to evaluate nerve tumors and inflammation, but generally is not needed in the setting of traumatic nerve injury[17], aside from its use for vascular suppression with 3D MRI techniques[28].

Using 3 Tesla clinical MRI scanners and phased-array surface coils, modern day strategies maximize nerve-to-background contrast and spatial resolution by applying fast spin-echo (FSE) T2-weighted sequences (echo time (TE) of ~80ms), with additional fat and flow suppression[29], including use of Dixon FSE[30] that takes advantage of the phase differential between spins at water and fat resonances. Since the introduction of these approaches, detailed anatomical images of nerve with enhanced characterization of pathology has been possible clinically and in the lab[27,31,32]. Discussed below are some new and emerging quantification methods, many that have been well validated in central nervous system imaging, and although residing in the realm of research at this time with none being standard care, many have the potential to mature into viable biomarkers and progress MRN's capability in assessing peripheral nerve health.

1.1.2 Three-Dimensional Analysis

3D-volume neurography and photograph-like images from cinematic rendering augment standard MRN[33]. The ability to rotate and view from any angle is not only diagnostically useful for radiologists, but also helpful in communicating results to referring clinicians[34]. Sequences such as 3D fast (turbo) spin-echo (FSE or TSE; vendor-specific acronyms include VISTA, SPACE, and CUBE) provide high-spatial and high-contrast resolution that enable detection and visualization of subtle alterations in nerve contour, signal intensity, and 3D nerve fascicular reconstruction[35]. The combination of diffusion-weighted (DW) sequences with 3D approaches has been championed the last few years, for instance in the form of DW reversed fast imaging with steady-state precession (3D DW-PSIF) sequences[21,35], although it has not yet been adopted widely in clinical practice or research, potentially due to added time and cost. Volumetric MRI of the dorsal root ganglia has been studied to determine if it is a valid non-invasive in-vivo measure of neuron loss after distal axotomy[36], finding good correlation to histology (r=0.67). Overall, 3D imaging does not replace 2D imaging due to less sharpness and lower in-plane (about 1mm compared to 0.4-0.5mm in 2D imaging, a significant difference)[37].

1.1.3 Diffusion Imaging

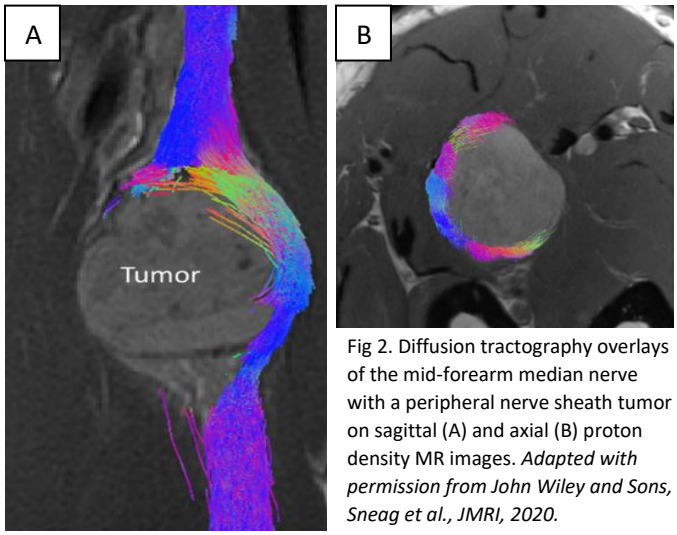

Fig 2. Diffusion tractography overlays of the mid-forearm median nerve with a peripheral nerve sheath tumor on sagittal (A) and axial (B) proton density MR images. *Adapted with permission from John Wiley and Sons, Sneag et al., JMRI, 2020.*

The application of diffusion weighted imaging (DWI) and most critically diffusion-tensor imaging (DTI) created much excitement in recent years because of its ability to interrogate nerve anisotropy. Anisotropy refers to the directional dependence of a physical measure. In the case of nerves, the tube-like character of fascicles, which preferentially restricts the naturally occurring Brownian motion of water molecules in the longitudinal plane, produces anisotropy that is detectable with these techniques. In addition to allowing selective nerve visualization, several derived parameters are readily quantifiable, including the apparent diffusion coefficient (ADC) and for DTI, fractional anisotropy (FA)[38–40], which allows inferences about orientation and tissue architectural organization[39,41,42]. Diffusion schemes in at least six "gradient" directions for DTI allows for the generation of 3D visualization (diffusion tensor tractography (DTT), Fig 2) of nerve fiber tracts[32,43,44]. DTT is one of the few diagnostic techniques that has been specifically assessed within the field of nerve regeneration through comparison with histological and functional parameters of recovery. It has been found capable of depicting tract termination at the injury site, as well as distal fiber growth, and also correlates with neurophysiological and functional recovery in humans[39,45–52]. Furthermore, mean FA has been shown to correlate well with the number of large axons within healthy, uninjured nerves[47], suggesting a potential role in donor nerve selection for nerve transfer surgery, although this finding requires corroboration and validation in injured nerve. Regeneration reestablishes both fascicular structure and myelination, and therefore anisotropy, resulting in progressively increasing FA and axial diffusivity (AD), and decreasing radial diffusivity (RD) values, while ADC and mean diffusivity (MD) values normalize as edema resolves[39,53]. DTI does not, however, appear to correlate with severity of axonal injury[47] and results obtained in the controlled environment of lab-based research, with the ability to study ex vivo or only straight nerve segments, have not translated to the more challenging case of in vivo clinical research or practice. Jeon et al.[54] reviewed some of the unique obstacles posed by peripheral nerve imaging that have impeded clinical uptake, including the challenges of spatial and contrast resolution, non-linear nature of nerves, off-isocenter imaging, before offering practical approaches to mitigate against these concerns. Improvements to signal-to-noise (SNR) using principal component analysis with generalized spherical deconvolution[55] may partially address the high variance in diffusion parameters within healthy and injured nerve, and across scanners[54]. Due to single-shot echo-planar sequences being so susceptible to even small inhomogeneities in the magnetic field with poorer fat suppression, Martín-Noguerol et al. found that non–single-shot echo-planar DTI aids significantly, especially in the more challenging clinical contexts associated with trauma and artifact[56,57]. Given the importance of vascularity in nerve injury and regeneration, recent approaches have sought to combine vascular (intravoxel incoherent motion (IVIM)) and DTI to depict both anisotropic microcirculation and microstructure simultaneously in rat sciatic nerve with some success[58,59]. Part of the importance of DTI is that it elucidates the microarchitecture of nerves from a very different vantage point and dimension to the more standard structural resolution of anatomic imaging techniques

because of its reliance on molecular movement associated with complex diffusion patterns within the nerve. Ultra-high field strength has been combined with DTI successfully, achieving a structural resolution of (0.2 x 0.2mm) while overcoming the DTI distortion artifacts associated with increasing field strengths[60]. Although significant hurdles exist and advancements in coil design, post processing, and pulse sequences are required[54], these parameters are some of the most intuitively appealing and may yield potentially useful biomarkers capable of robustly evaluating nerve degeneration and regeneration at depth in the near future including, axonal number and integrity[39,61].

1.1.4 Magnetic Susceptibility Imaging

Magnetic susceptibility[62] is an alternative key contrast mechanism that has predominantly been used to image the cerebral venous system and comes in two forms. Susceptibility-weighted imaging (SWI), signal dephasing near tissue interfaces, transformed bothersome susceptibility artefact into a method of enhancing contrast between tissues. Subsequently, the development of quantitative susceptibility mapping (QSM) allowed detailed charting of magnetic source characteristics[63], and has been used to evaluate myelin in the brain. The ability of QSM to quantify differences in iron deposition, myelin, and oxygen saturation suggests this may be a feasible marker of peripheral nerve health in certain circumstances. Detection of iron in macrophages or myelin may inform on Wallerian degeneration or detect an increase in myelin that might correspond with increasing axons and regeneration. However, this remains a nascent technique in peripheral nerve evaluation and requires additional refinement to address the small size of nerves and complicated phase behavior from interference from sources of susceptibility external to the nerves such as air-tissue interfaces, subcutaneous fat and bone, and intraneural lipid-equivalent tissues[63].

1.1.5 Magnetic Transfer

Magnetization transfer[64,65] (MT) generates tissue contrast based on magnetization exchange between free and restricted protons, represented by collagen, myelin, and axonal proteins. This makes it particularly interesting for measuring denervation and reinnervation and it has been shown to be a sensitive metric of myelin density changes caused by both demyelination and axonal loss[66–68]. Beyond simply axonal content and state of myelin, a sensitivity to collagen is of interest in chronic denervation states. Delays in nerve repair are frequent and the window of opportunity to reinnervate nerve and muscle is little more than a year[69]; the ability to detect collagenization[70] may help personalize treatment, preventing futile surgeries and missed opportunities. Nevertheless, the need for high spatial resolution and SNR when imaging peripheral nerve presents a particular challenge for quantitative measurements in nerve using MT imaging[37].

A multiparametric approach[56,63], overlaying and weighting the above MR nerve imaging approaches (such as DTI, SWI, MT) based on clinical context, as well as potentially post-processing of neural morphometrics[63], may provide a richer assessment of nerve health than any marker alone. Quantitative MRN parameters were assessed in SMA (spinal muscular atrophy) [71,72], including T2 relaxation time (increased), proton spin density (decreased), cross sectional area (decreased), with differences found to be clearly statistically significant, as well as correlation with neurophysiology. SMA is a different model of nerve health compared to the more common demyelinating, entrapment neuropathy, or nerve injury models. It represents only loss of motor axons, as also occurs in ALS (amyotrophic lateral sclerosis). Given that perhaps the majority of a nerve, even a motor nerve[73,74], is made up of non-motor axons, the significant differences found in SMA suggest even greater differences should be found in other models

that include sensory axon loss because pathological changes and tissue contrast will not be diluted or obscured by the presence of a great amount of unaffected sensory neural tissue and axons.

1.1.6 Nerve Selective Contrast Agents

The blood-nerve barrier (BNB) and subsequent lack of selectivity for nerve has hindered the utility of contrast in nerve evaluation. Conversely, the BNB could be used to identify areas of injury or where the BNB may be regenerating or degenerating; BNB breakdown encompasses the entire distal trunk in Wallerian degeneration, for instance, and repair appears to closely follow nerve outgrowth from the proximal stump[75]. To take advantage of this, contrast agents have been developed that accumulate selectively in nerve[76]. Gadofluorine M (GFM) accumulates in fibers undergoing Wallerian degeneration, fades with remyelination in parallel with regrowth of nerve fibers, and persists in non-regenerating nerve, which has clear implications for evaluating nerve regeneration. However, such contrast agents have not been approved by the US Food and Drug Administration (FDA).

Superparamagnetic iron oxide (SPIO) particles, including ultrasmall SPIO particles, are applied for cellular and molecular imaging because of their biocompatibility and ability to generate localized hypointenseT2 and T2* areas[77,78]. SPIO particles are rapidly phagocytized by macrophages, whose accumulation in nerve undergoing Wallerian degeneration can then be followed from day 1 to 8[77] before fading. Additional agents have been developed and some FDA approved including polyaminocarboxylate chelates, which induce hyperintense signal on T1-weighted MR images[35]. Some exciting advances include nanoparticles (nanoneurotracers) functionalized with an antibody for targeted deployment in combination with high field strength MRI[79–81]; these could be developed for selective imaging of multiple cell types[81]. Label-free imaging will always be preferable, but the selectivity and strength of signal achievable with safe and target-specific labels and contrast agents likely represents the field that will most advance resolution and quantification of nerve health, in particular in the lab, but with a trade-off clinically due to the delay associated with FDA approval.

1.2.1 Quantitative Muscle MR

As with Ultrasound (US) and EMG, evaluation of muscle acts as a surrogate marker of nerve injury due to denervation-related changes and is a highly useful complement to any assessment of nerve injury and regeneration[82–85]. On MRI, acute and subacute denervation demonstrates normal T1 but diffuse high intensity on T2 fluid-sensitive sequences because of increased extracellular fluid space (“edema pattern”), whose timing seems to parallel Wallerian denervation starting around 4 days, or even as soon as 24 hours in rats[24,86]. However, in chronic denervation, muscle precursor stems cells differentiate into adipose cells and fibroblasts[87], which results in increased T1 fatty signal, as well as atrophy. These characteristics, as well as changes in anisotropy secondary to reduced muscle fiber diameter[88], can be exploited to provide multiparametric quantitative measures (qMRI). Fat Fraction (FF), T2 mapping, apparent fiber diameter (AFD), and DTI/MT ratio of the muscle are all capable of providing *indirect* in vivo measures of axonal loss[67,82,83]. Nevertheless, further validation of each of the muscle MR parameters, as well as the multi-parametric approach, is required to characterize the longitudinal relationship between these muscle metrics and the state of the innervating nerve, as well as the muscle’s receptivity to being re-innervated. Collateral reinnervation is expected to warp the relationship between muscle signal and innervation status; up to 80% of axons may potentially be lost before collateral reinnervation fails and muscle fibers remain denervated[89,90].

Volumetric assessment of muscle has been recently found to be a responsive outcome measure of reinnervation when standardized to BMI (body mass index)[91]; it represents another quantitative surrogate marker of nerve health and could be used in conjunction with additional MR imaging biomarkers. Similar to chronic denervation of nerve, chronic denervation of muscle after a year or so appears to also result in such degeneration, atrophy, fibrosis, and fatty replacement that the muscle can no longer be reinnervated; however, there is some debate over whether it is the distal nerve or muscle itself that is primarily unreceptive to new axons[6]. Regardless, quantitative muscle biomarkers sensitive to change in the chronic period (between one and two years being the most clinically important[6,69]) would further address the clinical question of whether a repair would be futile or successful.

1.2.2 MR Elastography

MR elastography (MRE) offers similar benefits to US-based elastography methods discussed below but remains to be explored in the evaluation of peripheral nerve. Three requisite steps involve producing mechanical waves, adopting a modified phase-contrast MR sequence to image the wave, and applying an inversion algorithm to create an elastogram[92]. MRE has been applied in many organs, including the liver, brain, and muscle, but not in peripheral nerve likely due to limited spatial resolution that results from the reduced number of waves and volume averaging effects on the waves detected. In muscle[93], Basford et al. found stiffness to correlate with neuromuscular pathology as well as active contraction; however, this study only included one patient with peripheral nerve involvement (polio) and showed significant differences to muscles paralyzed by central lesions. The relationship of elastography with physical stiffness in nerve and muscle offers an interesting correlate to the tactile assessment of nerve intraoperatively that often guides surgeons subjectively in their assessment of nerve health.

1.3 Motor Unit MRI (MUMRI)

An approach using diffusion-weighted magnetic resonance imaging (MRI) has recently been combined with in-scanner electrical stimulation to image individual MUs[94,95], Fig 3. Its potential for detecting muscle reinnervation is exciting, allowing simultaneous surveillance of multiple muscles for the presence

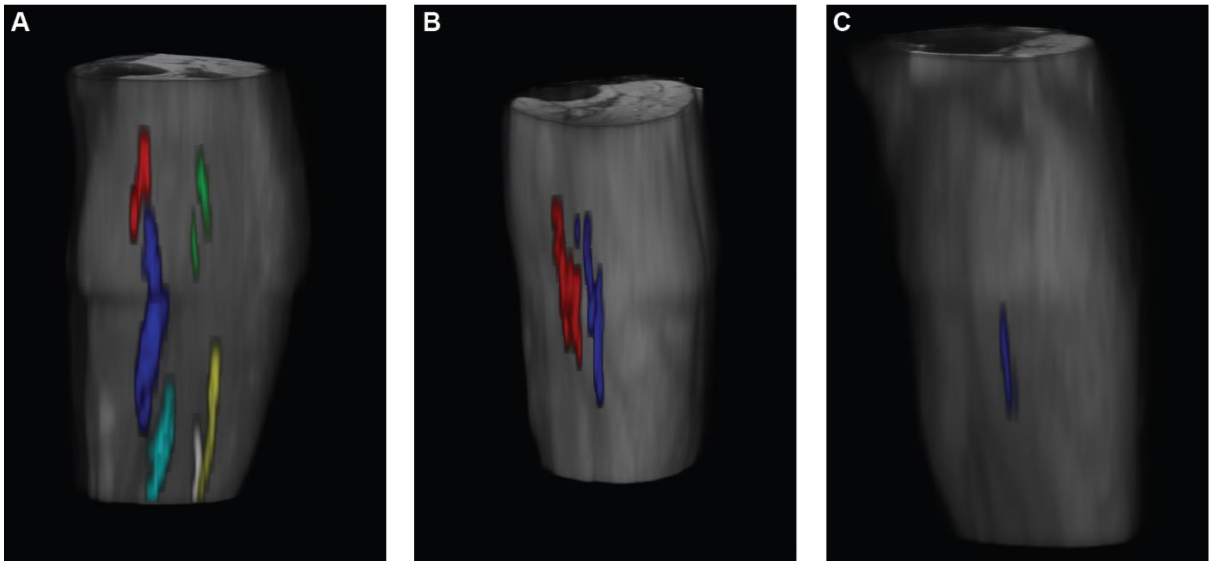

Fig 3. 3D motor unit MRI (MUMRI) of single motor units in the lower limbs of healthy volunteers. Liminal electrical stimulation was applied to the common peroneal nerve at the fibular head, and the 3D structure of up to six motor units was reconstructed from multi-slice DWI images sensitive to motor unit contraction. 3D MUMRI reveals a more complex human motor unit structure than previously thought, with several units splitting and re-forming along their length. *Heskamp et al., 2022, available via CC BY 4.0.*

of actively or passively stimulated MUs. This capability may allow for the detection of nascent MUs, or the detection of sparse residual MUs allowing for rapid and non-invasive confirmation of nerve in continuity over a wide field of view, both important for surgical decision making as well as quantifying motor nerve health and changes over time non-invasively. The relative size and shape of MUs might also be used as a surrogate for denervation in a conceptually similar way that EMG MU size correlates with denervation, although the fascicular or volumetric constraints of MU area may reduce validity of this approach.

Table 1. Summary of Magnetic Resonance (MR) Imaging Techniques at 3 Tesla Field Strength

Modality	Stage	Resolution/Metric	Advantages	Disadvantages	Select References
MRN	C	0.3-0.4mm (in-plane)	Provides high spatial resolution	Subjective	25–27,29–32
3D MRN	C	0.6-1mm (in-plane)	If obtained isotropically, can be easily reformatted into arbitrary planes	Less sharp compared to 2D imaging	21,33–37
DTI	E	01.5mm (in-plane)	Quantifies microstructural change, identifies tracts and fiber growth, FA may correlate with axon number	Lower spatial resolution compared to qualitative imaging; susceptible to distortion and field inhomogeneity	32,38–61
QSM	E	Signal intensity	Sensitive to myelin and iron (macrophages)	Poor resolution, interference	62,63
MT	E	Signal intensity	Sensitive to collagen, myelin, and axon proteins	Poor resolution	37,64–68,70
MR Contrast agents	E	Signal intensity	Detect WD	Not FDA approved, safety	35,76–81
MR Muscle quantification	E	Multiparametric continuous variables	Larger target tissue, less resolution needed, may correlate with receptivity of muscle to reinnervation	Surrogate for nerve, changes may reflect collateral reinnervation and disuse	24,67,82,83,86,88
MR Muscle volume	E	Volume in mm^3	Easily quantifiable	Surrogate for nerve, changes may reflect collateral reinnervation and disuse	91
MR Elastography	P	Single continuous variable in muscle; kPA or velocity.	May correlate with receptivity of muscle to reinnervation, may correlate with level of innervation	Surrogate for nerve, changes may reflect collateral reinnervation and disuse. Unclear if measurement of nerve is feasible due to resolution.	92,93
MUMRI	P	Unknown volume (mm^3) of MU detectable	Detection of nascent or residual MUs, quantifies over time, MU size	MU size anatomically constrained, activating non-standard or deeper muscles may be difficult	94,95

C: currently in clinic use for nerve; I: currently used intraoperatively for nerve; L: currently in lab use for nerve; E: emerging for nerve; P: potential but untested in nerve. MRN: MR neurography, 3D: 3 dimensional, 2D: 2 dimensional, DTI: diffusion tensor imaging, QSM: quantitative susceptibility mapping, MT: Magnetization Transfer, MUMRI: motor unit MRI, FA: fractional anisotropy, WD: Wallerian degeneration, MU: motor unit

2. ULTRASOUND BASED IMAGING TECHNIQUES

2.1 Neuromuscular Ultrasonography (NMUS)

As with MRI, technical advances in ultrasound hardware and signal processing are rapidly finding applications in neuromuscular medicine, research, and training[96–100]. Neuromuscular physicians and researchers have realized the significant benefits of ultrasound in evaluating nerves and muscles, including its widespread availability, low cost, high resolution, dynamic capability to explore large areas of nerves, and painlessness[97,101]. As a result, over the last few decades, ultrasound has been increasingly used standalone as well as contemporaneous with neurophysiology[98]. NMUS is presently used to obtain basic qualitative and quantitative measures of nerve and muscle such as echogenicity, the presence of nearby structural changes, and cross-sectional area. For the most part, pathological nerve cross-sectional area increases and its echogenicity decreases, while muscle, which can again be used as a surrogate for nerve health, atrophies and becomes more echogenic[98]. Unfortunately, beyond myelination abnormalities[102,103], routine ultrasound provides little information regarding the innervation state of a nerve, including Wallerian degeneration, regeneration, or axonal content. Fascicles within a nerve, appearing as a honeycomb in cross-section on ultrasound, can be easily identified, and in the early days of nerve ultrasonography researchers had hoped to exploit this characteristic and detect a relationship to axonal content. However, the observed fascicles represent a fraction of the true number, a difference exacerbated as probe frequency decreases[104,105]. Standard neuronal ultrasonographic characteristics vary little with Wallerian degeneration[104], chronic denervation[106,107], or reinnervation, perhaps because the most salient aspect of B-mode nerve imaging relies on scattering properties of the connective tissue enveloping the axons and not the axons themselves[104]. Unless degenerated or lost axons are replaced by material that scatters ultrasound signals in a distinctively different manner, or gross cross-sectional area changes commensurably, basic quantitative techniques will struggle to meaningfully quantify the level of denervation. As discussed below, new developments in objective quantitation are on the horizon that may be able to not only serve as biomarkers but also provide insights into pathophysiology.

2.2 Quantitative Muscle Ultrasound

Muscle ultrasound clinically is usually performed qualitatively, which again suffers from dependence on examiner experience and a lack of reliability. Quantification aims to first enhance reliability in detecting what is usually subjectively obvious, with the hope that this is followed by enhanced sensitivity and specificity. While the Heckmatt scale is occasionally used when semi-objectively quantifying muscle ultrasound images[108], it suffers from a subjective component, is not a continuous scale, and reliability has been questioned[109]. Nevertheless, muscle is substantially easier to examine than nerve using standard

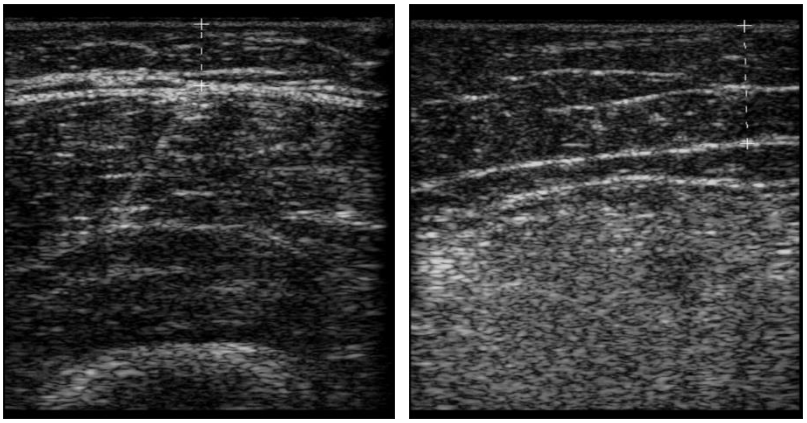

Fig 4. Left: normal muscle echogenicity. Right: severely denervated muscle echogenicity with increased subcutaneous tissue and obliteration of bone echo.

quantitative ultrasound techniques (Fig 4), such as those that rely on calibrated grayscale or backscatter imaging. Grayscale echo intensity is usually analyzed offline via simple computer-assisted grayscale histogram analysis. Originally, there was concern that compression of backscatter data into 256 grayscale levels by proprietary software resulted in unwanted bias; however, significant differences have not been found between methods employing backscatter and grayscale levels, resulting in most studies relying on the more accessible grayscale metric. These techniques estimate the acoustic energy reflected to the transducer[110–115], and calibration is always required for optimal standardization. Unfortunately, reference values are not only highly device-dependent, but they require much effort to obtain[109]. Simple and rapid standardization techniques have been attempted[116], but the variability of parameters involved in image generation between ultrasound machines restricts the application to longitudinal within subject studies using the same machine[116], and preferably the same examiner. Nevertheless, once proprietary algorithmic manipulation is removed, it appears reliability may be significantly improved[117]. This represents a promising avenue for improvement in quantitative muscle ultrasound. As discussed below, other methods have yielded positive results beyond standard mean grayscale analysis.

2.2.1 Ultrasound of denervated muscle

Although fewer studies have assessed the performance of quantitative ultrasound in denervated muscle (predominantly ALS) compared to primary muscle pathologies, relationships have been found between the level of pathology and echointensity[111–114,118]. Unlike MRI, ultrasound is unfortunately not able to detect early edema seen in denervation[119]. In general, studies attempt to predict the presence, absence, and category of muscle disease[120], and far fewer have explicitly focused on the level of muscle denervation, which would be the most relevant marker for nerve health. In this regard, initial findings with more advanced methods have managed to detect differences in muscle type and gender, using higher-order texture abstractions that rely upon spatial variations of pixel intensities to reflect muscle microstructure, being less susceptible to device characteristics.[121,122]

2.2.2 Heterogenous muscle signal in ultrasound

Heterogeneity of muscle echo intensity has not been explored significantly. This may be important for nerve injury and regeneration, which can have patchy involvement of axons innervating any given muscle due to neural architecture inhibiting nerve growth outside of a MU's territory or across fascicular boundaries[6] in severely denervated muscle (moth-eaten pattern). Visually depicting the echo intensity throughout the muscle as a topographical map, with hills of different heights and areas, it becomes possible to quantify areas affected rather than simply the mean echointensity across the entire muscle that is less sensitive to changes in muscle fiber innervation. As discussed earlier, the potential for a muscle to lose most of its innervation before collateral reinnervation fails[89,90] renders ultrasound less sensitive to peripheral nerve injury or degeneration compared to primary muscle disease, but it may be able to inform in the early stages of reinnervation or late stages of denervation.

2.2.3 Dynamic ultrasound imaging

Already established in the detection of fasciculations[115,123,124], and quantifiable using speckle tracking of tissue motion[125], dynamic ultrasound imaging has the unique potential to comment on the presence of nascent units (small motor units currently undergoing reinnervation)[126] and fibrillations[127–129], albeit with the small size of both being a complicating factor[130,131]. Such an approach might augment or even replace components of the EMG study when reviewing for muscle reinnervation; compared to needle EMG, its ability to rapidly review multiple muscles in their entirety and avoid the limitation of EMG's

small sampling area and invasiveness strongly favor the use of dynamic ultrasound if feasible[115,123]. Similar to the superiority of US over EMG in detecting fasciculations[132], the combination of US with EMG significantly increased the chances of detecting residual MUs after nerve trauma[133], a finding vital to preventing unnecessary surgery and likely improving outcomes. This was followed by further enhanced sensitivity in MU detection using nerve stimulation in addition to US guided EMG[134]. No comparative studies have been performed between EMG and ultrasound in detecting nascent units; despite the smaller size of nascent MUs, the combination of US and EMG, potentially also with stimulation, will likely outperform standard EMG alone. The presence or absence of motor units is not the only information that speckle tracking of tissue motion may provide. Akin to the concept of MUMRI discussed above, if quantifiable, the *anatomical* size of individual motor units might be informative in a conceptually similar manner to the information contained within the size of its electrical MUP counterpart measured with EMG; although, if collateral reinnervation does not cross fascicular boundaries[135], this relationship will be distorted.

2.2.4 Ultrasound Muscle Elastography

B-mode imaging provides information on acoustic impedance, structure, and motion of a muscle; however, beyond the field of neuromuscular evaluation, the technique of ultrasound elastography is widely used to assess in real-time the mechanical properties of tissues, including stiffness[136]. Denervated muscle histology changes over time, with healthy muscle replaced by connective tissue and fat, progressively becoming more difficult to reverse over a year or two[6,137]. It has been hypothesized these histological changes translate into differences in stiffness detectable by elastography[109]. Some of the main elastography techniques and related studies in denervated muscle are briefly discussed below.

Strain elastography[138–141] (SE) uses speckle pattern tracking to quantify tissue deformation after applying pressure. The lack of pressure information (elastic modulus) and subjective grading are significant disadvantages compared to other techniques. Few studies in denervated muscle or nerve have been performed, with some promise seen when evaluating muscle in ALS, although no significant correlation to nerve health was found in carpal tunnel syndrome[140].

Acoustic radiation force impulse (ARFI) imaging is based on similar principles to strain elastography[142]; however, it overcomes the lack of a standardized pressure pulse by implementing a fixed focused ultrasound “push” beam, which consists of a prolonged burst of pulses[143]. Nevertheless, because the stress produced by ARFI is unknown, output images are again qualitative maps of tissue. Furthermore, data acquisition can be limited due to overheating caused by the substantial power requirement to produce the push beam[143]. A form of ARFI, the Viscoelastic Response[144], can be used to measure muscle fiber direction through muscle anisotropy. To our knowledge, neither of these techniques appears to have been studied in denervated muscle.

Sheer Wave Elastography (SWE) overcomes the limitations associated with both the applied stress and objective measurement (Fig 5). A push beam like ARFI is used to generate a shear wave inside the tissue. The propagating shear wave is tracked using pulse-echo techniques and shear wave velocity is estimated by solving the shear wave equations using advanced mathematic modeling[145], calculation of stiffness[146,147] (tissue modulus), and generation of quantitative shear wave velocity maps. There are drawbacks, including muscle anisotropy requiring the transducer to be oriented longitudinally along the muscle, otherwise accuracy and reliability suffer[148]. This becomes particularly problematic when we consider the variability of muscle pennation, which makes it challenging to ensure correct orientation.

On the flip side, such anisotropy might represent a useful biomarker if it correlates with levels of denervation, or chronicity of denervation, and would be an interesting avenue to explore further.

While predominantly studied in primary muscle disease[143], several studies have also evaluated SWE of muscle in focal nerve entrapment and motor neuron disease[120,149,150], with mixed results due to high variance in healthy tissue, a lack of reference values, and variability between machines[150]. Stiffness

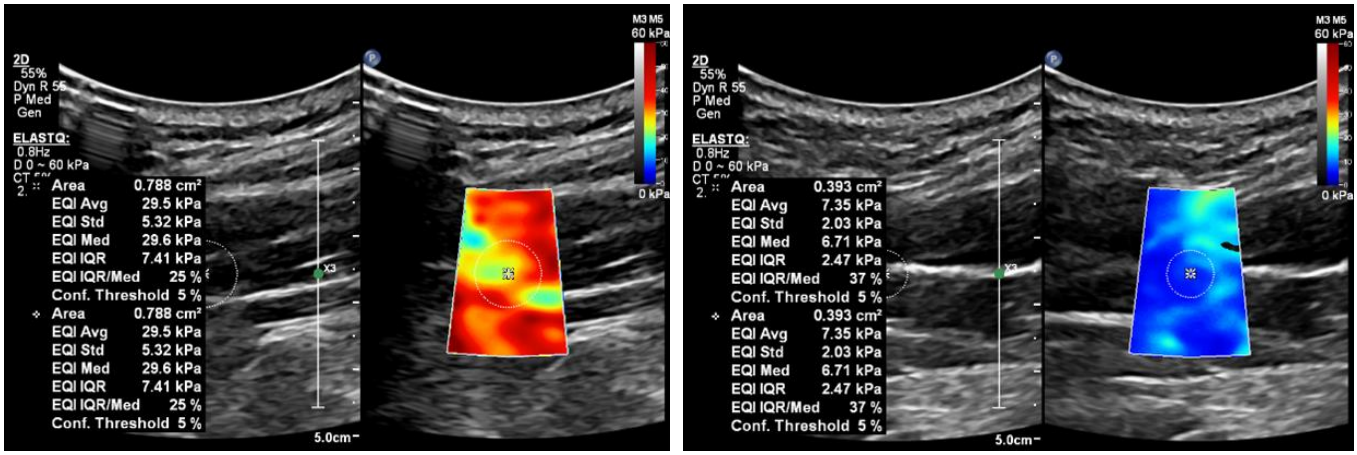

Fig 5: Muscle Ultrasound. Left: trapezius under contraction. Right: Same muscle relaxed. kPA: kilopascal.

echogenicity matrix (SEM)[151] is a recent novel approach looking to leverage complementary characteristics of two modalities; SWE and B-mode echo intensity. Research into the use of both SWE and B-mode imaging in evaluating muscle remains in its infancy, but a multiparametric approach may represent a more viable path forward in the evaluation of nerve health using muscle SWE given the described limitations of each modality individually.

2.3 Quantitative Nerve Ultrasound

Compared to muscle, there is significantly less research into applying advanced ultrasound techniques to nerve, but it is coming. As mentioned, this paucity of research stems from the small caliber of nerves, the architecture of their connective tissue, and the limits of resolution of commercial scanners. However, several groups are actively advancing quantitative ultrasound neurography[152].

Akin to quantitative muscle ultrasound, backscatter and grayscale approaches have successfully distinguished between normal and pathological nerves at a group level, particularly in entrapment syndromes and diabetic polyneuropathy (DPN), and especially when examining ratios between fascicular and non-fascicular tissue termed “nerve density”[153–155]. Although intraneural quantitative methods have not been found superior to simple gross nerve cross-sectional area measurements in detecting the presence of entrapment neuropathies[156], Tagliafico did show a relationship between median nerve hypointensity and severity of carpal tunnel syndrome (CTS), which may relate to increased edema rather than change in axonal content[157]. Most studies to date are focused on detecting the presence or absence of a pathology (entrapment neuropathy or polyneuropathy, usually), and few quantify the severity of pathology or level of innervation. Beyond standard grayscale quantitation, the future of quantitative nerve ultrasound may lie more in several technologies discussed below.

Of note, techniques based on ultrasound stimulation[158] are discussed in the companion review of the same subject focused on neurophysiology because of the associated neuromodulation and the generation of action potentials; although, discussion of this interesting field could equally reside in this

review. Additionally, while beyond the scope of this review, it is worth mentioning that ultrasound's versatility and accessibility mean that it is commonly used as an adjunct in the evaluation of nerve health - for instance, to locate nerve for needle electrode placement during neurophysiologic assessment of nerve (stimulation and recording).

2.3.1 Ultra-High Frequency Ultrasound (UHF-US) of Nerve

Beyond improved fascicular identification[105], ultra-high-resolution ultrasound of nerves (Fig 6) has rarely been studied. Frequencies are generally described as being between 30 and 100 MHz[159], although no agreed threshold exists, and resolution as high as 20µm[159–161], as compared to standard clinic based ultrasounds with 10MHz probes at around 150µm, 100µm with 17MHz probes, and 73µm with 22MHz probes, at shallow depths[162,163]. However, recently, Brya[164] examined the correlation of intra-fascicular 30-MHz ultrasound backscatter-based coefficients to collagen and myelin content in cadaver ulnar nerve fascicles. Moderately good correlation was found between backscatter and collagen (0.56), less so with myelin (0.2), but highest when combined (0.68). Similar findings using the gray-level co-occurrence matrix suggest this approach may also be applied without access to RF data[164]. Given the limited penetration depth of UHF-US, its importance may ultimately lie intraoperatively, either stand-alone or potentially as a component of multi-modal photoacoustic techniques discussed below[165,166]. Although studies remain pending, should they be able to provide information such as that related to axonal content, changes along a nerve suggestive of regeneration, or outline intact fascicles within neuromas, there would be immediate clinical and research utility.

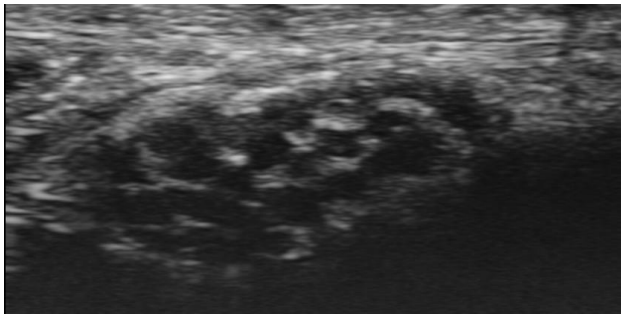

Fig 6: 70 MHz Ultra-high frequency ultrasound image of median nerve at the wrist showing individual fascicles.

2.3.2 Ultrasound Nerve Elastography

The last few years have seen significant interest in the potential of elastography to comment on nerve pathology, especially for the mechanical changes associated with entrapment neuropathies and polyneuropathy[152,167]. The sensitivity and specificity of SWE (Fig 7) and strain elastography are higher than CSA for diabetic polyneuropathy, with high reproducibility[168–172]. However, it is unclear whether the severity of neuropathy correlates highly with SWE values, which histological changes result in elastography changes, and whether these findings are likely to translate to other pathologies such as denervation and regeneration. Furthermore, complexity in using SWE has been highlighted by several studies[173–177] which demonstrated SWE measurements vary depending on where along the nerve the measurement is taken, whether in transverse lor longitudinal axis, which nerve is measured, and gender, but not significantly by age, BMI, weight, or height. Furthermore, tensile force, limb position, depth, device platform, and ROI size also impact measurements[177–183], and the effect of nerve diameter is likely significant once a threshold is met due to fewer shear wavelengths and volume effects[152,176]. The numerous elastography studies in CTS have had varying results[152,184]. Although a pilot study using strain elastography in CTS did not show significant correlation[140], several have looked at SWE in CTS, finding slightly less diagnostic ability than CSA and variable correlation with severity[185–190]. A modest

improvement of clinimetrics was seen when US metrics were combined, with application of intra-nerve comparison[186,187,191,192]. Given the wide range of values in healthy individuals, the merit of SWE when

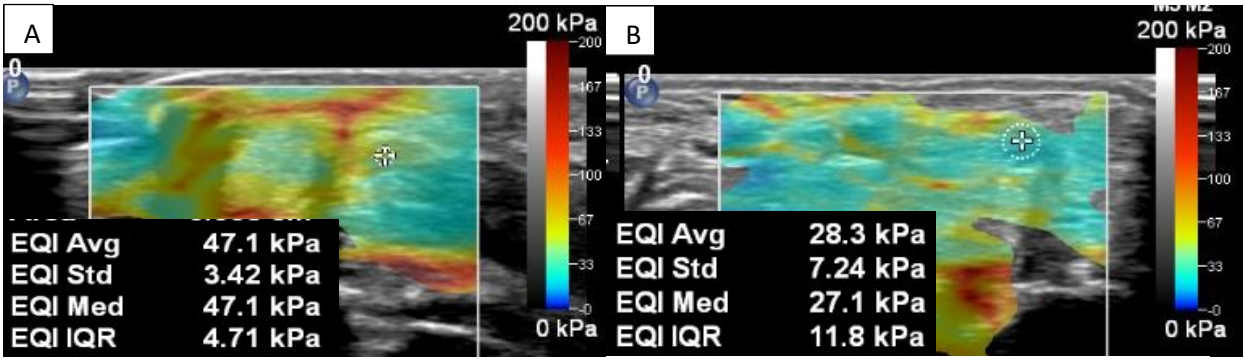

Fig 7: *Cross-sectional SWE image of completely denervated median nerve at the wrist (A), and contralateral unaffected median nerve at the wrist (B), revealing pressure difference in KPa. Long axis measurements showed similar results, as did alterations in size of the region of interest. Median nerve area also differed, 6.3mm (A) versus 10.5mm (B). kPA: kilopascal.*

evaluating nerve health may be in the longitudinal evaluation at the same location and in the same individual, or between groups of subjects. Using an intra-subject reference, more subtle changes that are associated with denervation or regeneration, such as histological alterations arising from new axonal growth, may be detectable and quantifiable. Recent animal sciatic crush studies demonstrated a remarkably tight correlation in SWE measurements longitudinally after sciatic crush[193,194], slowly increasing in stiffness over time, despite the arrival of axons in the later time periods (8 weeks). In this study, the ratio of the elastic modulus between measurements taken pre and post injury was used for intra-subject standardization, akin to ultrasound measurements for carpal tunnel syndrome assessing the CSA ratio between wrist and forearm[195]. Additionally, there appeared to be little variation in ratio between the rodents within each group (standard deviation of 0.06) suggesting standardization to proximal nerve segment resulted in high reliability. These results appear generally more promising than studies in human nerve entrapment and polyneuropathy and the use of the crush injury model may be more valid in neuroregeneration research. However, characterizing SWE changes in different contexts will be important going forward, including until full reinnervation has completed and in chronic denervation states, as well as at different tissue depths.

2.3.3 Vascular and Contrast-enhanced Ultrasound

Standard color and power doppler ultrasound is unable to detect the slow flow within the microcirculation of nerve tissue[196]. However, advances in Doppler (e.g., superb microvascular imaging) now permit the assessment of vascular changes in nerve[188,191,197–200]. Intraneural hypervascularity may be caused by compression or inflammatory response, which is usually graded subjectively. When quantification via image-processing has been applied, intraneural vascularity correlated well with the severity of neuropathy[188,201]. Intraneural vascular changes in Wallerian degeneration and the reinnervating growth cone have not been studied to our knowledge, and it is unclear if the perfusion and energy requirements within chronically denervated nerve are significantly different from a nerve with a full complement of axons, which may allow a further metric of nerve health. High-frequency contrast-enhanced US using microbubbles of inert gas has also successfully quantified peripheral nerve perfusion[196], which may turn out to be relevant in detecting vascular growth associated with regenerating nerve or even correlate with axon density. In a study into neurovascular coupling, the trigeminal ganglion was examined using microbubble tracking and a 15MHz ultrasound probe with an

ultrafast neuroimager, showing a significant hemodynamic response following afferent activation (corneal nociceptive)[202]. This is interesting because the number of neurons that needed to be activated for a hemodynamic response to be detected was low (about 300 neurons) and suggests the neurovascular coupling of distal peripheral nerve might be able to be assessed similarly to sensory ganglia at such a detailed level.

Table 2. Summary of Ultrasound based Imaging Techniques, including Photoacoustic Imaging

Modality	Stage	Resolution/Metric	Advantages	Disadvantages	Select References
QUS Muscle	E	0.1-0.15mm	Easy to quantify, texture analysis promises higher sensitivity	Machine and operator dependent, collateral reinnervation obscures denervation level	109–118,120–122
Dynamic US	E	0.1-0.15mm, high frame rate allows fibrillation detection, Speckle tracking	Detection of residual or nascent units, possibly fibrillations	Non-target muscle movement obscuring target muscle movement	115,123–134
SWE Muscle	E	Kilopascal or velocity, greater than millimeter scale	Quantifies muscle stiffness important for receptivity to nerve	Reliability, many factors affect measurements, reference values lacking, collateral reinnervation obscures denervation level	109,120,136,143,148–151
UHF-US Nerve	E	0.073-0.1mm,	Higher resolution than MRI if superficial, distinguish fascicles, correlates with collagen and myelin, intraoperative use	Resolution reduces with depth more than a few centimeters	153–157,165,166
SWE Nerve	E	Kilopascal or velocity, greater than millimeter scale	Metric related to nerve mechanical properties, detects changes associated with WD	Reliability, many factors affect measurements, reference values lacking	152,167–179,181–194,203
CEUS	E	Assesses flow within intraneural microvessels	Improved resolution compared to doppler US	Need for contrast injection, untested in nerve injury	196
Doppler US, SMI	E	Assesses flow within intraneural microvessels	Vascular changes correlate with nerve health and WD	Surrogate marker, ordinal semi-objective quantification, low sensitivity, untested in nerve injury	188,191,197–199,201
PAI	E	4-400µm depending on ultrasound transducer	Structural, molecular, and functional information, high resolution	Portability, economic viability, restricted depth of imaging	204–221

C: currently in clinic use for nerve; I: currently used intraoperatively for nerve; L: currently in lab use for nerve; E: emerging for nerve; P: potential but untested in nerve. QUS: quantitative ultrasound, WD: Wallerian degeneration, CEUS: contrast enhanced US, SMI: superb microvascular imaging.

3. Photoacoustic Imaging (PAI)

Since uncovering the property of "sonorousness" inherent in different materials when exposed to rapidly-interrupted sunlight and the creation of a "*Photophone*" (Alexander Graham Bell[222]), it has been found that any wave in the electromagnetic spectrum is capable of inducing sound in tissue (acoustic

waves). Optical energy (electromagnetic waves) can be absorbed by molecules and subsequently converted into heat, resulting in thermoelastic expansion. It is this movement that creates sound waves that can be detected by ultrasound transducers. The combination of optical energy and acoustic measurement has been described in several ways; perhaps the most graphic being Bell's "Photophone", but more recently the most common terms are "photoacoustic" and "optoacoustic", although "thermoacoustic" describes the general effect of sound induction through thermal expansion. Further nomenclature that has arisen depends on the resolution obtained, field of view, frequencies and exogenous contrast agents used, with additional common descriptors[204,205] including tomography, macroscopy, mesoscopy, microscopy, multispectral, label-free etc., the details of which are covered in several excellent reviews[204,206,223–229].

The scalability of PAI has found an important role in bridging the sizeable gap between imaging modalities that lie on the more invasive end of the spectrum, such as fluorescence microscopy, and those less invasive techniques such as the previously discussed MRI and US modalities. PAI can ultimately be thought of as an extension of US imaging albeit using a novel signal source and underlying contrast mechanism; pulse-echo ultrasonography utilizes the mismatch in impedance between soft tissues to image structures, whereas PAI utilizes the different characteristics of light-absorbing soft-tissue chromophores. This means that PAI can capture not only structural features but importantly extends to molecular and functional features[207]. Sound scatters far less than light in soft tissue, perhaps 1000 times less[230], and as such the acoustic signal suffers significantly lower attenuation to allow much greater depth of high resolution imaging; a near infrared window (NIR; 700–1700 nm) enables tissue penetration depth up to several centimeters.[225] The resulting resolution remains limited by the attenuation of high-frequency ultrasonic waves in tissue, which results in a practical depth-to-resolution ratio of up to 200[231]; for example, at a depth of 5mm, resolution could be as high as 25µm[208,209].

PAI systems can be categorized via which optical illumination and acoustic detection methods are being combined. PAI *Macroscopy*[207] is capable of imaging up to several centimeters, relying on a non-focused optical beam over a wider area and with detection in the range up to 10 MHz, with resolution up to 100µm. PAI *Mesoscopy*[207,210,211] is similar in process but images up to several millimeters with resolution achieved through increased ultrasonic frequency detection, up to 200 MHz with a resolution generally found to be in the range of 50-100µm; although, some report up to 4 µm axially 18 µm transverse with depths up to as much as 5 mm[208]. With the only difference between PAI macroscopy and PAI mesoscopy being the transducer, this means that macroscopy and mesoscopy can readily be switched, allowing easy scalability with little need to change equipment – a significant bonus for translatability to the clinical environment. The third category is Photoacoustic *Microscopy*; it is considered beyond the scope of this review due to the imaging depth being so low, but it is briefly described for the sake of completeness. PAI microscopy is generally limited to sub-millimeter depths and utilizes an alternate method of illumination that systematically moves a focused beam across the target (relying on optical resolution, rather than acoustic resolution in macroscopy and mesoscopy), with each area detected separately by the ultrasound transducer, which removes the need for tomographic techniques. Resolution in this category of PAI can be down to the sub-micron level[212].

Contrast in PAI has been shown to be a consequence of endogenous optical absorbers, including lipid, lipofuscin, melanin, collagen, water, and hemoglobin[213,214]. The inclusion of lipid in this list of endogenous chromophores is of interest due to the myelin component of peripheral nerve[217,220,221]. In particular, the potential for measuring changes in the combination of endogenous chromophores such

as lipid[232], vascularity/hemaglobin[219], water, and collagenization within nerve offers exciting but as yet mostly untapped future possibilities for evaluating nerve health and denervation in the acute and chronic stages, importantly including Wallerian degeneration, chronic denervation, and regeneration. Only a few studies have focused specifically on peripheral nerve evaluation and PAI[215–221]. Matthews et al. demonstrated peripheral nerve imaging proof-of-concept by imaging ex-vivo mouse sciatic nerve embedded in chicken tissue. Although at submillimeter depths, resolution was measured as 41µm, and the endogenous chromophore (contrast agent) was found to be the lipid content of the myelin. This is encouraging for the measurement of regeneration and degeneration given the close relationship of myelination to axon number, growth, and degeneration. Another study used multispectral laser excitation, which adds to the resolution and specificity of PAI by localizing specific chromophores due to differential light absorption characteristics[206]. Li et al.[220] applied this multispectral PAI and demonstrated a penetration depth up to 2.7cm; in this study, the group noted an axial resolution of 124µm when performing in-vivo imaging in rodent at a depth of 2mm.

Endogenous chromophores are most preferable but are limited and often lack precision due to weak optical absorption[225], but exogenous chromophores are being developed at a rapid rate in attempts to increase contrast of tissue[223,225,229]. Although peripheral nerve represents a challenge due to the blood-nerve barrier[233], headway is being made[223]. As previously described, impermeability to contrast can be used to highlight areas where the blood-nerve barrier has been disrupted, which is helpful in detecting Wallerian degeneration and potentially neuronal growth cones; alternatively, it can potentially be opened via various mechanisms to allow for contrast agent uptake[234] and the imaging of intraneural structural and molecular properties.

3.1 Obstacles and Future advances in PAI

PAI has numerous limitations and much scope for continued advancement in the field of peripheral nerve imaging. The practicalities of creating a portable and economically viable system represents a significant barrier but will be key for adoption rates. One approach to overcome this is focused on low cost light emitting diodes (LED) to replace expensive lasers[235]. Traditional piezoelectric transducers have put some constraints on PAI systems[236] and studies have investigated improving the practicality of a PAI system through the use of optical sensors; including transparent Fabry–Perot sensors in the place of piezo transducers to allow simultaneous illumination of tissue and detection of ultrasound without the transducer obscuring the laser[237], as well as aid in miniaturization and reduction of interference[238]. Optimal image processing is a necessity for effective imaging using PAI and represents its own challenges. Here too, improvements are being made including algorithms to quantify images more effectively through use of artificial intelligence and machine learning to extract as much information as possible from the signal[229,239–243].

In attempts to improve resolution of PAI, several methods have been applied with some success[224]. Localization-based approaches (localization optoacoustic tomography) uses rapid sequential acquisition of 3D photoacoustic images to achieve sub-diffraction (below diffraction limits of the wavelength of light used) spatial resolution and reduce artifact[244]. The inherent scattering nature of light within biological tissues presents a substantial obstacle on the penetration depth of non-scattered photons[245]. Using "wavefront shaping"[245,246] to compensate for scattering, improvements of up to ten times in signal-to-noise and six times sub-acoustic resolution have been achieved. Finally, the acoustic diffraction limit has also been surpassed by using techniques that achieved super-resolution in microscopy[247] (super-resolution fluorescence fluctuation microscopy), which induced temporal fluctuations of fluorescence

using “blinking” fluorescence molecules. This approach was translated to PAI with good effect by exploiting multiple random speckle illuminations as the source of acoustic fluctuations[248].

Advances in optical, ultrasonic, and image processing technology, along with the ability to image structural, molecular, and functional features, have resulted in PAI becoming one the most exciting and fast improving modalities in non-invasive imaging at greater than millimeter depths. Improved targeting and resolution of contrast agents that are endogenous to nerve, or design of safe exogenous neural contrast agents, promises to provide unparalleled access to nerve health.

4. Multimodal Methods

4.1 Positron Emission Tomography (PET)

Damaged nerves uptake FDG-PET due to higher levels of metabolic demand from injury as well as increased firing rates[249], yielding another promising imaging biomarker of nerve health. Interesting avenues of ongoing research include neuronal-selective contrast agents, rather than relying on metabolic demand, and the necessary combination with other modalities such as CT or MRI for enhanced spatial resolution[250–252] that may have potential to inform on neuronal regeneration and degeneration. The combination of modalities not only increases neuronal structural resolution but also overlays another vital feature of nerve health, function, similar to photoacoustic techniques discussed above and highlights the benefit of dual modality approaches to imaging beyond just high-resolution structural detail.

4.2 Ultrasound Fusion

Medical image fusion involves overlaying images, or displaying side by side, from different imaging modalities after an initial co-registration and has gained widespread use in several medical specialties[253]. The combination of the two modalities (ultrasound images fused and co-located with pre-recorded MRI or CT images) not only allows practical guidance to obtain accurate recordings from otherwise hard to assess deep nerve and muscle, but also enables multimodal quantification of precisely located neuronal and muscular tissue, useful for assessing nerve health. Precisely stimulating and recording from deep nerve is challenging even with ultrasound guidance, but the combination with MRI overcomes this issue and augments the potential to assess nerve throughout the body. Fusion imaging represents the technological frontier of the ever closer relationship between neuromuscular ultrasound and neurophysiology, both in clinic and intra-operatively[254–256].

4.3 PAI Fusion

Pre-clinical studies have into multi-modal imaging of PAI with MRI[257] and ultrasound[216,228,258] have been demonstrated in recent years. Like PET fusion approaches, the goal is to exploit the complementary information provided by anatomical landmark imaging with the molecular and functional contrast offered by PAI. This has been used primarily in imaging gliomas to obtain clear borders, but the translatability to nerve is clear as shown by Ishihara in the evaluation of diabetic nerve[216]; the combination of rapidly acquired gross structure with molecular content would be invaluable for assessing nerve health, making clinical decisions, and monitoring treatment effects on investigational regenerative therapies.

5. In-Vivo Lab and Intraoperative Imaging

5.1 MR Microneurography

Animal peripheral nerve imaging options expand beyond those available to humans and this offers distinct advantages and opportunities for improvement. For instance, high-resolution MR microneurography optimizes the spatial resolution of neurography images, using very high magnetic fields, extremely powerful gradients, and specific coils[259]. With a 9.4 Tesla scanner and gradients of 400mT/m, images of anatomical parts can be obtained with a spatial resolution of up to 30µm[259–262], far superior to clinical MRI resolution of approximately 0.4-0.5mm[263], and several times greater than in-human microneurography methods, even with highly-restricted field of view, of a little over 100µm[264,265]; although, SNR may be improved further in human studies using new acceleration methods[266,267]. Such high resolution may detect intraneural structure at a level relevant to axonal content and nerve health evaluation, akin to a magnetic resonance nerve biopsy.

As mentioned, application of MR microneurography using 3 T scanners using a restricted field of view was capable of enough visualization of internal nerve structure to allow quantification nerve fascicle area, as well as perineurium and epineurium area, using a segmentation protocols[264,268]. These areas were combined into a ratio (fascicle to nerve ratio), potentially relating to nerve pathology given significant correlation to demyelinating pathology[268]. Discussed below, this is a similar theme to fascicular ratios applied in ultrasound and are based on the rationale that different compartments within nerve differentially respond to pathological processes, providing reliable intraneural structural metrics beyond simply whole nerve cross-sectional area. The application to nerve evaluation would involve only a small segment of nerve being evaluated ("biopsied") to understand in maximal possible detail the health of the nerve for clinical or surgical decision-making, or to accurately monitor degeneration, regeneration, and response to neurotherapeutics.

5.2 Ultra-High Frequency Ultrasound

The sonographic counterpart of MR Microneurography is the previously described UHF-US (section 2.3.1), also termed micro-ultrasound[165], and similar to US biomicroscopy[269–271] (UBM) that has historically been applied in embryology research and subsequently ophthalmology, angiology, and dermatology. Limitations with mechanically scanned transducers have been overcome using phased array layouts[271] allowing the dedicated high-frequency probes from 30 to 100 MHz and more[159,160] to increase the spatial resolution to the micron level (as low as 20 µm), albeit at the expense of the investigation depth due to previously described inherent depth-to-resolution ratio of up to 200[105,159,231]. The appropriateness of which ultrasound machine is used differs depending on environment, as exemplified by recent technological advances in clinical research machines allowing for ultra-high to low (70-1MHz) imaging capabilities (*Vevo F2 Fujifilm Visualsonics*). Such increased freedom of data access with open architecture, high performance multimodal imaging, and quantitative interfaces offers the opportunity for significantly more sophisticated techniques to be applied in controlled and laboratory environments.

5.3 Photoacoustic Alternative Forms of Microscopy

Photoacoustic techniques reviewed above are applicable to, and perhaps best suited to, in-vivo animal research. However, as mentioned, significant development of the systems and techniques are required. This review focuses predominantly on the more non-invasive peripheral nerve imaging techniques that are capable of depths of at least several millimeters. However, it is important to at least point to the

advances in numerous microscopy imaging techniques that are applicable at very shallow depths (millimeter and below), which have exploded in recent years[233] and include categories such as optical microscopy[272–275] and optical coherence tomography[276] with and without florescence[277–282] or labelling[233], as well as micro-CT[283,284] and spectroscopy[285,286]. Although considered beyond the scope of this review, microscopy as a field has evolved far enough to require its own dedicated review focused on invasive and ex-vivo imaging techniques for the evaluation of peripheral nerve health, degeneration, and regeneration.

5.4. Intraoperative

The opportunity for direct access to nerve intraoperatively offers the opportunity for quite different approaches to imaging, as well as greater resolution of modalities discussed already, such as intraoperative ultrasound. Some techniques have already started to be applied clinically with several emerging techniques at varying stages of development in the translational spectrum.

Neuromuscular ultrasound has found its place firmly in the outpatient clinic, not least the neurophysiology lab due to the real-time addition of a structural correlate to concurrent electrophysiological and clinical exam findings, and overlap in required anatomical knowledge[287,288]. In line with increasing interest in intraoperative peripheral nerve neurophysiology[289], the natural extension of this is into the intraoperative environment; direct access to nerve and muscle without intervening tissue harnesses the full power of the highest frequencies. Recognition of its applicability intraoperatively is rising steadily in the era of ultra-high frequencies[290–292], as well as its vascular and sonoelastographic capabilities, and the argument for its place alongside intraoperative neurophysiology is beginning to look similar to that of its clinic-based counterpart. The most obvious application is that of ultra-high frequency ultrasound, with resolution up to 30µm using commercially available devices (*VevoMD, Fujifilm Visualsonics*). Current benefits of its application intraoperatively are already manifold including, nerve identification and mapping, and visualizing fascicular level detail to maximally spare healthy tissue in delicate surgical approaches to peripheral nerve tumors and neuromas[104,159,290,291,293–297]. If echotexture parameters can be discovered that indicate levels of denervation or collagenization, then this would amplify its use immediately intraoperatively in evaluating nerve health, especially in nerve injury surgery and exploration. Elastography of nerve, as discussed above, has shown promise in evaluating nerve health and represents an intuitively appealing modality in peripheral nerve surgery. Frequently, the firmness and texture of nerve, taken to be a surrogate for collagenization and fibrosis, is subjectively determined by the surgeon in evaluating viability of nerve tissue; elastography speaks directly to this firmness via evaluation of propagating wave velocity within the intraneural tissue. However, as discussed above in section 2.3.2, there is a way to go before sensitive and specific information can be extracted from ultrasonographic elastography signals of nerve. The degree, type, and distribution of vascular changes are associated with nerve in different states of degeneration and regeneration, and this could be an important biomarker of nerve health[298,299]. One potential approach to evaluating this potentially valid metric is intraoperatively with microvascular ultrasonography[191,300,301]. Such microvascular assessment could potentially also be attempted pre-operatively through use of clinic-based ultrasound (discussed above), MR imaging[298], or laser doppler techniques[302], but the access provided intraoperatively allows enhanced resolution and offers a potential final check before committing to the often nerve-racking and irreversible transection of a nerve.

In section 3, we discussed PAI and its application to the evaluation of nerve health. Intraoperative use[215,303] again takes advantage of the depth-to-resolution acoustic properties in PAI, greatly enhancing likely resolution, similar to ultra-high frequency ultrasound but with reported potential resolution even higher, approaching 4 μm[208]. This level of resolution at sufficient depth with the added molecular and potentially functional information provided by the differential tissue responses to thermoelastic stress make PAI theoretically an ideal candidate for intraoperative use; as long as practicalities of integrating acoustic and optical components be overcome in the challenging environment [215,304,305] (discussed above). Although discussed in the companion review focused on neurophysiology, it is worth also noting here the intraoperative potential of electrical impedance tomography (EIT). This is an imaging modality that benefits from direct access to nerve and provides the capability to image fascicular level depolarization at resolutions below 200μm[306,307]. In addition to the proposed role in neuromodulation, especially of the vagus nerve, identifying fascicles that require repair in partial nerve injuries has long been a problem in peripheral nerve surgery and would significantly help in recovery of function through encouraging fascicular repair while also aiding in avoiding morbidity from unnecessary repairs.

7. Conclusion

The recent substantial increase in awareness from both clinical and research communities of the promise of non-invasive nerve imaging is driving its rapid evolution across multiple modalities and specialties. To unleash the exciting promise offered by so many imaging techniques identified and discussed in this scoping review, advances in technology are needed to occur in tandem to achieve the hoped-for exponential improvement in powerful and responsive imaging biomarker and outcome measures to expedite progress in both neurotherapeutics and clinical practice. Many measures of nerve health discussed in this review have seen high variance within healthy individuals, impacting their value as a biomarker. Overcoming this will undoubtedly rely on technological advances but taking advantage of combining modalities and techniques may represent low hanging fruit that can be rapidly exploited to enhancement precision in the evaluation of nerve health.

The present scoping review serves as a complement to Part 1, which specifically concentrates on non-neurophysiology [11]. Some modalities straddle neurophysiology and imaging but have only been covered by one of the reviews (such as EIT and ultrasound stimulation being covered within Part 1). Within the combined reviews, we have covered an extensive assemblage of current and promising non-invasive imaging and neurophysiological approaches, aiming to guide both the planning of peripheral neuroregeneration research as well as the optimization of patient care. In addition to aiding in the selection of appropriate metrics of nerve health, we have highlighted what we believe to be important areas of promise and necessary avenues for further research.

References

1. Bailey, R., Kaskutas, V., Fox, I., Baum, C. M. & Mackinnon, S. E. Effect of upper extremity nerve damage on activity participation, pain, depression, and quality of life. *J. Hand Surg.* **34**, 1682–1688 (2009).

2. Pain and Quality of Life Following Nerve Injury | 2010-10-01 | AHC…. *Relias Media | Online Continuing Medical Education | Relias Media - Continuing Medical Education Publishing* https://www.reliasmedia.com/articles/20685-pain-and-quality-of-life-following-nerve-injury.

3. Ciaramitaro, P. *et al.* Traumatic peripheral nerve injuries: epidemiological findings, neuropathic pain and quality of life in 158 patients. *J. Peripher. Nerv. Syst. JPNS* **15**, 120–127 (2010).

4. England, J. D. & Asbury, A. K. Peripheral neuropathy. *Lancet Lond. Engl.* **363**, 2151–2161 (2004).

5. Martyn, C. N. & Hughes, R. A. Epidemiology of peripheral neuropathy. *J. Neurol. Neurosurg. Psychiatry* **62**, 310–318 (1997).

6. Gordon, T. Peripheral Nerve Regeneration and Muscle Reinnervation. *Int. J. Mol. Sci.* **21**, 8652 (2020).

7. Bazarek, S. *et al.* Spinal motor neuron transplantation to enhance nerve reconstruction strategies: Towards a cell therapy. *Exp. Neurol.* 114054 (2022) doi:10.1016/j.expneurol.2022.114054.

8. Ghergherehchi, C. L. *et al.* Polyethylene glycol (PEG) and other bioactive solutions with neurorrhaphy for rapid and dramatic repair of peripheral nerve lesions by PEG-fusion. *J. Neurosci. Methods* **314**, 1–12 (2019).

9. Lanier, S. T., Hill, J. R., Dy, C. J. & Brogan, D. M. Evolving Techniques in Peripheral Nerve Regeneration. *J. Hand Surg.* **46**, 695–701 (2021).

10. Carvalho, C. R., Oliveira, J. M. & Reis, R. L. Modern Trends for Peripheral Nerve Repair and Regeneration: Beyond the Hollow Nerve Guidance Conduit. *Front. Bioeng. Biotechnol.* **7**, (2019).

11. Mandeville, R. *et al.* A Scoping Review of Current and Emerging Techniques for Evaluation of Peripheral Nerve Health, Degeneration, and Regeneration: Part 1, Neurophysiology. Manuscript Submitted for Publication. (2023).

12. Bramer, W. M., Rethlefsen, M. L., Kleijnen, J. & Franco, O. H. Optimal database combinations for literature searches in systematic reviews: a prospective exploratory study. *Syst. Rev.* **6**, 245 (2017).

13. Wood, M. D., Kemp, S. W. P., Weber, C., Borschel, G. H. & Gordon, T. Outcome measures of peripheral nerve regeneration. *Ann. Anat. - Anat. Anz.* **193**, 321–333 (2011).

14. Tricco, A. C. *et al.* PRISMA Extension for Scoping Reviews (PRISMA-ScR): Checklist and Explanation. *Ann. Intern. Med.* **169**, 467–473 (2018).

15. JBI Manual for Evidence Synthesis - JBI Global Wiki. https://jbi-global-wiki.refined.site/space/MANUAL.

16. Singh, T. & Kliot, M. Imaging of peripheral nerve tumors. *Neurosurg. Focus* **22**, 1–10 (2007).

17. Grant, G. A. *et al.* The utility of magnetic resonance imaging in evaluating peripheral nerve disorders. *Muscle Nerve* **25**, 314–331 (2002).

18. Bendszus, M. & Stoll, G. Technology Insight: visualizing peripheral nerve injury using MRI. *Nat. Clin. Pract. Neurol.* **1**, 45–53 (2005).

19. Stoll, G., Wilder-Smith, E. & Bendszus, M. Imaging of the peripheral nervous system. in *Handbook of Clinical Neurology* vol. 115 137–153 (Elsevier, 2013).

20. Kermarrec, E. *et al.* Ultrasound and Magnetic Resonance Imaging of the Peripheral Nerves: Current Techniques, Promising Directions, and Open Issues. *Semin. Musculoskelet. Radiol.* **14**, 463–472 (2010).

21. Chhabra, A. *et al.* MR Neurography: Past, Present, and Future. *Am. J. Roentgenol.* **197**, 583–591 (2011).

22. Deshmukh, S. & Samet, J. Ultrasonography of Peripheral Nerves. in *Atlas of Ultrasound-Guided Procedures in Interventional Pain Management* (ed. Narouze, S. N.) 289–296 (Springer, 2018). doi:10.1007/978-1-4939-7754-3_30.

23. Tan, E. T. *et al.* Quantitative MRI Differentiates Electromyography Severity Grades of Denervated Muscle in Neuropathy of the Brachial Plexus. *J. Magn. Reson. Imaging JMRI* **n/a**, 1104–1115 (2022).

24. Bendszus, M., Koltzenburg, M., Wessig, C. & Solymosi, L. Sequential MR Imaging of Denervated Muscle: Experimental Study. *Am. J. Neuroradiol.* **23**, 1427–1431 (2002).

25. Filler, A. G. *et al.* Magnetic resonance neurography. *Lancet Lond. Engl.* **341**, 659–661 (1993).

26. Magnetic Resonance Neurography - Howe - 1992 - Magnetic Resonance in Medicine - Wiley Online Library. https://onlinelibrary.wiley.com/doi/abs/10.1002/mrm.1910280215.

27. Cudlip, S. A., Howe, F. A., Griffiths, J. R. & Bell, B. A. Magnetic resonance neurography of peripheral nerve following experimental crush injury, and correlation with functional deficit. *J. Neurosurg.* **96**, 755–759 (2002).

28. Sneag, D. B. *et al.* Post-Contrast 3D Inversion Recovery Magnetic Resonance Neurography for Evaluation of Branch Nerves of the Brachial Plexus. *Eur. J. Radiol.* **132**, 109304 (2020).

29. Filler, A. G., Maravilla, K. R. & Tsuruda, J. S. MR neurography and muscle MR imaging for image diagnosis of disorders affecting the peripheral nerves and musculature. *Neurol. Clin.* **22**, 643–682 (2004).

30. Tan, E. T. *et al.* Improved nerve conspicuity with water-weighting and denoising in two-point Dixon magnetic resonance neurography. *Magn. Reson. Imaging* **79**, 103–111 (2021).

31. Vargas, M. I. *et al.* New approaches in imaging of the brachial plexus. *Eur. J. Radiol.* **74**, 403–410 (2010).

32. Sneag, D. B. & Queler, S. Technological Advancements in Magnetic Resonance Neurography. *Curr. Neurol. Neurosci. Rep.* **19**, 75 (2019).

33. Möller, I., Miguel, M., Bong, D. A., Zaottini, F. & Martinoli, C. The peripheral nerves: update on ultrasound and magnetic resonance imaging. *Clin. Exp. Rheumatol.* **36 Suppl 114**, 145–158 (2018).

34. Deshmukh, S., Tegtmeyer, K., Kovour, M., Ahlawat, S. & Samet, J. Diagnostic contribution of contrast-enhanced 3D MR imaging of peripheral nerve pathology. *Skeletal Radiol.* **50**, 2509–2518 (2021).

35. Eppenberger, P., Andreisek, G. & Chhabra, A. Magnetic Resonance Neurography. *Neuroimaging Clin. N. Am.* **24**, 245–256 (2014).

36. West, C. A. *et al.* Volumetric magnetic resonance imaging of dorsal root ganglia for the objective quantitative assessment of neuron death after peripheral nerve injury. *Exp. Neurol.* **203**, 22–33 (2007).

37. Chhabra, A. *et al.* MR Neurography: Advances. *Radiol. Res. Pract.* **2013**, 1–14 (2013).

38. van der Jagt, P. K. N. *et al.* Architectural configuration and microstructural properties of the sacral plexus: A diffusion tensor MRI and fiber tractography study. *NeuroImage* **62**, 1792–1799 (2012).

39. Martín Noguerol, T., Barousse, R., Socolovsky, M. & Luna, A. Quantitative magnetic resonance (MR) neurography for evaluation of peripheral nerves and plexus injuries. *Quant. Imaging Med. Surg.* **7**, 398–421 (2017).

40. Martín Noguerol, T. & Barousse, R. Update in the evaluation of peripheral nerves by MRI, from morphological to functional neurography. *Radiologia* **62**, 90–101 (2020).

41. Simon, N. G., Lagopoulos, J., Gallagher, T., Kliot, M. & Kiernan, M. C. Peripheral nerve diffusion tensor imaging is reliable and reproducible: Reliability of Peripheral Nerve DTI. *J. Magn. Reson. Imaging* **43**, 962–969 (2016).

42. Cervantes, B. *et al.* Isotropic resolution diffusion tensor imaging of lumbosacral and sciatic nerves using a phase-corrected diffusion-prepared 3D turbo spin echo: Phase Corrected 3D TSE DTI of Lower Back Nerves. *Magn. Reson. Med.* **80**, 609–618 (2018).

43. Hiltunen, J. *et al.* Pre- and post-operative diffusion tensor imaging of the median nerve in carpal tunnel syndrome. *Eur. Radiol.* **22**, 1310–1319 (2012).

44. Skorpil, M., Karlsson, M. & Nordell, A. Peripheral nerve diffusion tensor imaging. *Magn. Reson. Imaging* **22**, 743–745 (2004).

45. Takagi, T. *et al.* Visualization of peripheral nerve degeneration and regeneration: Monitoring with diffusion tensor tractography. *NeuroImage* **44**, 884–892 (2009).

46. Lehmann, H. C., Zhang, J., Mori, S. & Sheikh, K. A. Diffusion tensor imaging to assess axonal regeneration in peripheral nerves. *Exp. Neurol.* **223**, 238–244 (2010).

47. Boyer, R. B. *et al.* 4.7-T diffusion tensor imaging of acute traumatic peripheral nerve injury. *Neurosurg. Focus* **39**, E9 (2015).

48. Simon, N. G. *et al.* Visualizing axon regeneration after peripheral nerve injury with magnetic resonance tractography. *Neurology* **83**, 1382–1384 (2014).

49. Meek, M. F., Stenekes, M. W., Hoogduin, H. M. & Nicolai, J.-P. A. In vivo three-dimensional reconstruction of human median nerves by diffusion tensor imaging. *Exp. Neurol.* **198**, 479–482 (2006).

50. Gallagher, T. A., Simon, N. G. & Kliot, M. Diffusion tensor imaging to visualize axons in the setting of nerve injury and recovery. *Neurosurg. Focus* **39**, E10 (2015).

51. Farinas, A. F. *et al.* Diffusion Magnetic Resonance Imaging Predicts Peripheral Nerve Recovery in a Rat Sciatic Nerve Injury Model: *Plast. Reconstr. Surg.* **145**, 949–956 (2020).

52. Farinas, A. F. *et al.* Diffusion tensor tractography to visualize axonal outgrowth and regeneration in a 4-cm reverse autograft sciatic nerve rabbit injury model. *Neurol. Res.* **41**, 257–264 (2019).

53. Andersson, G., Orädd, G., Sultan, F. & Novikov, L. N. In vivo Diffusion Tensor Imaging, Diffusion Kurtosis Imaging, and Tractography of a Sciatic Nerve Injury Model in Rat at 9.4T. *Sci. Rep.* **8**, 12911 (2018).

54. Jeon, T., Fung, M. M., Koch, K. M., Tan, E. T. & Sneag, D. B. Peripheral nerve diffusion tensor imaging: Overview, pitfalls, and future directions. *J. Magn. Reson. Imaging* **47**, 1171–1189 (2018).

55. Sneag, D. B. *et al.* Denoising of diffusion MRI improves peripheral nerve conspicuity and reproducibility. *J. Magn. Reson. Imaging* **51**, 1128–1137 (2020).

56. Martin Noguerol, T. *et al.* Functional MR Neurography in Evaluation of Peripheral Nerve Trauma and Postsurgical Assessment. *Radiographics* **39**, 427–446 (2019).

57. Martín-Noguerol, T., Montesinos, P., Barousse, R. & Luna, A. *RadioGraphics* Update: Functional MR Neurography in Evaluation of Peripheral Nerve Trauma and Postsurgical Assessment. *RadioGraphics* **41**, E40–E44 (2021).

58. Merchant, S., Yeoh, S., Mahan, M. A. & Hsu, E. W. Simultaneous Quantification of Anisotropic Microcirculation and Microstructure in Peripheral Nerve. *J. Clin. Med.* **11**, 3036 (2022).

59. Abdullah, O. M. *et al.* Orientation dependence of microcirculation-induced diffusion signal in anisotropic tissues: Organized Capillary Flow and Diffusion-Weighted Signal. *Magn. Reson. Med.* **76**, 1252–1262 (2016).

60. Schmid, A. B. *et al.* Feasibility of Diffusion Tensor and Morphologic Imaging of Peripheral Nerves at Ultra-High Field Strength. *Invest. Radiol.* **53**, 705–713 (2018).

61. Sheikh, K. A. Non-invasive imaging of nerve regeneration. *Exp. Neurol.* **223**, 72–76 (2010).

62. Haacke, E. M., Xu, Y., Cheng, Y.-C. N. & Reichenbach, J. R. Susceptibility weighted imaging (SWI). *Magn. Reson. Med.* **52**, 612–618 (2004).

63. Chen, Y., Haacke, E. M. & Li, J. Peripheral nerve magnetic resonance imaging. *F1000Research* **8**, F1000 Faculty Rev-1803 (2019).

64. Wolff, S. D. & Balaban, R. S. Magnetization transfer contrast (MTC) and tissue water proton relaxation in vivo. *Magn. Reson. Med.* **10**, 135–144 (1989).

65. Giorgetti, E. *et al.* Magnetic Resonance Imaging as a Biomarker in Rodent Peripheral Nerve Injury Models Reveals an Age-Related Impairment of Nerve Regeneration. *Sci. Rep.* **9**, 13508 (2019).

66. Dortch, R. D., Dethrage, L. M., Gore, J. C., Smith, S. A. & Li, J. Proximal nerve magnetization transfer MRI relates to disability in Charcot-Marie-Tooth diseases. *Neurology* **83**, 1545–1553 (2014).

67. Morrow, J. M. *et al.* MRI biomarker assessment of neuromuscular disease progression: a prospective observational cohort study. *Lancet Neurol.* **15**, 65–77 (2016).

68. Fan, S.-J. *et al.* Feasibility of quantitative ultrashort echo time (UTE)-based methods for MRI of peripheral nerve. *NMR Biomed.* **31**, e3948 (2018).

69. Brown, J. M., Shah, M. N. & Mackinnon, S. E. Distal nerve transfers: a biology-based rationale. *Neurosurg. Focus* **26**, E12 (2009).

70. Vuorinen, V., Siironen, J. & Röyttä, M. Axonal regeneration into chronically denervated distal stump. *Acta Neuropathol. (Berl.)* **89**, 209–218 (1995).

71. Kollmer, J. *et al.* Quantitative MR neurography biomarkers in 5q-linked spinal muscular atrophy. *Neurology* **93**, e653–e664 (2019).

72. Kollmer, J. *et al.* Magnetization transfer ratio: a quantitative imaging biomarker for 5q spinal muscular atrophy. *Eur. J. Neurol.* **28**, 331–340 (2021).

73. Bromberg, M. B. The motor unit and quantitative electromyography. *Muscle Nerve* **61**, 131–142 (2020).

74. Gesslbauer, B. *et al.* Axonal components of nerves innervating the human arm: Arm Nerve Axonal Components. *Ann. Neurol.* **82**, 396–408 (2017).

75. Seitz, R. J. *et al.* The blood–nerve barrier in Wallerian degeneration: A sequential long-term study. *Muscle Nerve* **12**, 627–635 (1989).

76. Bendszus, M. *et al.* Assessment of nerve degeneration by gadofluorine M-enhanced magnetic resonance imaging: Nerve Regrowth Assessed by MRI. *Ann. Neurol.* **57**, 388–395 (2005).

77. Bendszus, M. & Stoll, G. Caught in the Act: *In Vivo* Mapping of Macrophage Infiltration in Nerve Injury by Magnetic Resonance Imaging. *J. Neurosci.* **23**, 10892–10896 (2003).

78. Chen, M.-W. *et al.* Monitoring of macrophage recruitment enhanced by Toll-like receptor 4 activation with MR imaging in nerve injury: MRI of Enhanced Macrophage Recruitment in Nerve Injury. *Muscle Nerve* **58**, 123–132 (2018).

79. Deddens, L. H., Van Tilborg, G. A. F., Mulder, W. J. M., De Vries, H. E. & Dijkhuizen, R. M. Imaging Neuroinflammation after Stroke: Current Status of Cellular and Molecular MRI Strategies. *Cerebrovasc. Dis.* **33**, 392–402 (2012).

80. Tereshenko, V. *et al.* MR Imaging of Peripheral Nerves Using Targeted Application of Contrast Agents: An Experimental Proof-of-Concept Study. *Front. Med.* **7**, 613138 (2020).

81. Janjic, J. M. & Gorantla, V. S. Peripheral Nerve Nanoimaging: Monitoring Treatment and Regeneration. *AAPS J.* **19**, 1304–1316 (2017).

82. Tan, E. T., Zochowski, K. C. & Sneag, D. B. Diffusion MRI fiber diameter for muscle denervation assessment. *Quant. Imaging Med. Surg.* **12**, 80–94 (2022).

83. Argentieri, E. C. *et al.* Quantitative T_2 -mapping magnetic resonance imaging for assessment of muscle motor unit recruitment patterns. *Muscle Nerve* **63**, 703–709 (2021).

84. Lisle, D. & Johnstone, S. Usefulness of muscle denervation as an MRI sign of peripheral nerve pathology. *Australas. Radiol.* **51**, 516–526 (2007).

85. Kamath, S., Venkatanarasimha, N., Walsh, M. A. & Hughes, P. M. MRI appearance of muscle denervation. *Skeletal Radiol.* **37**, 397–404 (2008).

86. West, G. A. *et al.* Magnetic resonance imaging signal changes in denervated muscles after peripheral nerve injury. *Neurosurgery* **35**, 1077–1085; discussion 1085-1086 (1994).

87. Agley, C. C., Rowlerson, A. M., Velloso, C. P., Lazarus, N. R. & Harridge, S. D. R. Human skeletal muscle fibroblasts, but not myogenic cells, readily undergo adipogenic differentiation. *J. Cell Sci.* **126**, 5610–5625 (2013).

88. Holl, N. *et al.* Diffusion-weighted MRI of denervated muscle: a clinical and experimental study. *Skeletal Radiol.* **37**, 1111–1117 (2008).

89. Shefner, J. M. Motor unit number estimation in human neurological diseases and animal models. *Clin. Neurophysiol.* **112**, 955–964 (2001).

90. Stalberg, E. V. Macro electromyography, an update. *Muscle Nerve* **44**, 292–302 (2011).

91. Wilcox, M. *et al.* Volumetric MRI is a promising outcome measure of muscle reinnervation. *Sci. Rep.* **11**, 22433 (2021).

92. Low, G., Kruse, S. A. & Lomas, D. J. General review of magnetic resonance elastography. *World J. Radiol.* **8**, 59–72 (2016).

93. Basford, J. R. *et al.* Evaluation of healthy and diseased muscle with magnetic resonance elastography. *Arch. Phys. Med. Rehabil.* **83**, 1530–1536 (2002).

94. Birkbeck, M. G., Heskamp, L., Schofield, I. S., Blamire, A. M. & Whittaker, R. G. Non-invasive imaging of single human motor units. *Clin. Neurophysiol.* **131**, 1399–1406 (2020).

95. Heskamp, L. *et al.* In vivo 3D imaging of human motor units in upper and lower limb muscles. *Clin. Neurophysiol.* **141**, 91–100 (2022).

96. Cartwright, M. S. *et al.* A randomized trial of diagnostic ultrasound to improve outcomes in focal neuropathies. *Muscle Nerve* **52**, 746–753 (2015).

97. Zaidman, C. M., Seelig, M. J., Baker, J. C., Mackinnon, S. E. & Pestronk, A. Detection of peripheral nerve pathology. *Neurology* **80**, 1634–1640 (2013).

98. Walker, F. O., Cartwright, M. S., Wiesler, E. R. & Caress, J. Ultrasound of nerve and muscle. *Clin. Neurophysiol.* **115**, 495–507 (2004).

99. Tawfik, E. A. *et al.* Guidelines for neuromuscular ultrasound training. *Muscle Nerve* **60**, 361–366 (2019).

100. Carroll, A. & Simon, N. Current and future applications of ultrasound imaging in peripheral nerve disorders. *World J. Radiol.* **12**, 101–129 (2020).

101. Cartwright, M. S. & Walker, F. O. Neuromuscular ultrasound in common entrapment neuropathies. *Muscle Nerve* **48**, 696–704 (2013).

102. Zaidman, C. M. & Pestronk, A. Nerve size in chronic inflammatory demyelinating neuropathy varies with disease activity and therapy response over time: a retrospective ultrasound study. *Muscle Nerve* **50**, 733–738 (2014).

103. Beekman, R. *et al.* Ultrasonography shows extensive nerve enlargements in multifocal motor neuropathy. *Neurology* **65**, 305–307 (2005).

104. Silvestri, E. *et al.* Echotexture of peripheral nerves: correlation between US and histologic findings and criteria to differentiate tendons. *Radiology* **197**, 291–296 (1995).

105. Cartwright, M. S., Baute, V., Caress, J. B. & Walker, F. O. Ultrahigh-frequency ultrasound of fascicles in the median nerve at the wrist. *Muscle Nerve* **56**, 819–822 (2017).

106. Cartwright, M. S., Walker, F. O., Griffin, L. P. & Caress, J. B. Peripheral nerve and muscle ultrasound in amyotrophic lateral sclerosis: Ultrasound in ALS. *Muscle Nerve* **44**, 346–351 (2011).

107. Hobson-Webb, L. D. Neuromuscular ultrasound in polyneuropathies and motor neuron disease. *Muscle Nerve* **47**, 790–804 (2013).

108. Heckmatt, J. Z., Leeman, S. & Dubowitz, V. Ultrasound imaging in the diagnosis of muscle disease. *J. Pediatr.* **101**, 656–660 (1982).

109. Wijntjes, J. & van Alfen, N. Muscle ultrasound: Present state and future opportunities. *Muscle Nerve* **63**, 455–466 (2021).

110. Pillen, S. *et al.* Quantitative skeletal muscle ultrasound: Diagnostic value in childhood neuromuscular disease. *Neuromuscul. Disord.* **17**, 509–516 (2007).

111. Zaidman, C. M., Connolly, A. M., Malkus, E. C., Florence, J. M. & Pestronk, A. Quantitative ultrasound using backscatter analysis in Duchenne and Becker muscular dystrophy. *Neuromuscul. Disord.* **20**, 805–809 (2010).

112. Jansen, M. *et al.* Quantitative muscle ultrasound is a promising longitudinal follow-up tool in Duchenne muscular dystrophy. *Neuromuscul. Disord.* **22**, 306–317 (2012).

113. Simon, N. G. *et al.* Quantitative ultrasound of denervated hand muscles. *Muscle Nerve* **52**, 221–230 (2015).

114. Zaidman, C. M., Holland, M. R., Anderson, C. C. & Pestronk, A. Calibrated quantitative ultrasound imaging of skeletal muscle using backscatter analysis. *Muscle Nerve* **38**, 893–898 (2008).

115. Alfen, N. van & Mah, J. K. Neuromuscular Ultrasound: A New Tool in Your Toolbox. *Can. J. Neurol. Sci.* **45**, 504–515 (2018).

116. Wu, J. S., Darras, B. T. & Rutkove, S. B. Assessing spinal muscular atrophy with quantitative ultrasound. *Neurology* **75**, 526–531 (2010).

117. O'brien, T. G., Cazares Gonzalez, M. L., Ghosh, P. S., Mandrekar, J. & Boon, A. J. Reliability of a novel ultrasound system for gray-scale analysis of muscle: Muscle Ultrasound Reliability. *Muscle Nerve* **56**, 408–412 (2017).

118. Roy, B. *et al.* Exploring the relationship between electrical impedance myography and quantitative ultrasound parameters in Duchenne muscular dystrophy. *Clin. Neurophysiol.* **130**, 515–520 (2019).

119. Albano, D., Aringhieri, G., Messina, C., De Flaviis, L. & Sconfienza, L. M. High-Frequency and Ultra-High Frequency Ultrasound: Musculoskeletal Imaging up to 70 MHz. *Semin. Musculoskelet. Radiol.* **24**, 125–134 (2020).

120. van Alfen, N., Gijsbertse, K. & de Korte, C. L. How useful is muscle ultrasound in the diagnostic workup of neuromuscular diseases? *Curr. Opin. Neurol.* **31**, 568–574 (2018).

121. Martínez-Payá, J. J. *et al.* Quantitative Muscle Ultrasonography Using Textural Analysis in Amyotrophic Lateral Sclerosis. *Ultrason. Imaging* **39**, 357–368 (2017).

122. Molinari, F., Caresio, C., Acharya, U. R., Mookiah, M. R. K. & Minetto, M. A. Advances in Quantitative Muscle Ultrasonography Using Texture Analysis of Ultrasound Images. *Ultrasound Med. Biol.* **41**, 2520–2532 (2015).

123. Regensburger, M., Tenner, F., Möbius, C. & Schramm, A. Detection radius of EMG for fasciculations: Empiric study combining ultrasonography and electromyography. *Clin. Neurophysiol.* **129**, 487–493 (2018).

124. Grimm, A. *et al.* Muscle ultrasonography as an additional diagnostic tool for the diagnosis of amyotrophic lateral sclerosis. *Clin. Neurophysiol.* **126**, 820–827 (2015).

125. Goutman, S. A. *et al.* Speckle tracking as a method to measure hemidiaphragm excursion. *Muscle Nerve* **55**, 125–127 (2017).

126. Pelosi, L. & Heiss-Dunlop, W. Muscle ultrasound detects subclinical early reinnervation. *Clin. Neurophysiol.* **131**, 594–595 (2020).

127. Alfen, N. V., Nienhuis, M., Zwarts, M. J. & Pillen, S. Detection of fibrillations using muscle ultrasound: Diagnostic accuracy and identification of pitfalls. *Muscle Nerve* **43**, 178–182 (2011).

128. Pillen, S. *et al.* Muscles alive: Ultrasound detects fibrillations. *Clin. Neurophysiol.* **120**, 932–936 (2009).

129. van Baalen, A. & Stephani, U. Fibration, fibrillation, and fasciculation: say what you see. *Clin. Neurophysiol. Off. J. Int. Fed. Clin. Neurophysiol.* **118**, 1418–1420 (2007).

130. Bokuda, K. *et al.* Relationship between EMG-detected and ultrasound-detected fasciculations in amyotrophic lateral sclerosis: A prospective cohort study. *Clin. Neurophysiol.* **131**, 259–264 (2020).

131. Regensburger, M. Which kinds of fasciculations are missed by ultrasonography in ALS. *Clin. Neurophysiol.* **131**, 237–238 (2020).

132. Regensburger, M., Tenner, F., Möbius, C. & Schramm, A. P 157 Detection radius of EMG for fasciculations: combined ultrasonographic-electromyographic analysis. *Clin. Neurophysiol.* **128**, e404 (2017).

133. Gentile, L. *et al.* Ultrasound guidance increases diagnostic yield of needle EMG in plegic muscle. *Clin. Neurophysiol.* **131**, 446–450 (2020).

134. Padua, L. *et al.* Ultrasound-guided-electromyography in plegic muscle: Usefulness of nerve stimulation. *Muscle Nerve* **n/a**, 204–207 (2023).

135. Stålberg, E. Macro EMG, a new recording technique. *J. Neurol. Neurosurg. Psychiatry* **43**, 475–482 (1980).

136. Frulio, N. & Trillaud, H. Ultrasound elastography in liver. *Diagn. Interv. Imaging* **94**, 515–534 (2013).

137. MacKay, B. J. *et al.* Evidence-Based Approach to Timing of Nerve Surgery. *Ann. Plast. Surg.* **87**, e1–e21 (2021).

138. Ewertsen, C., Carlsen, J. F., Christiansen, I. R., Jensen, J. A. & Nielsen, M. B. Evaluation of healthy muscle tissue by strain and shear wave elastography – Dependency on depth and ROI position in relation to underlying bone. *Ultrasonics* **71**, 127–133 (2016).

139. Kim, S. J., Park, H. J. & Lee, S. Y. Usefulness of strain elastography of the musculoskeletal system. *Ultrason. Ultrason.* **35**, 104–109 (2015).

140. Martin, M. J. B. & Cartwright, M. S. M. A Pilot Study of Strain Elastography in the Diagnosis of Carpal Tunnel Syndrome. *J. Clin. Neurophysiol.* doi:10.1097/WNP.0000000000000334.

141. Martínez-Payá, J. J., del Baño-Aledo, M. E., Ríos-Díaz, J., Fornés-Ferrer, V. & Vázquez-Costa, J. F. Sonoelastography for the Assessment of Muscle Changes in Amyotrophic Lateral Sclerosis: Results of a Pilot Study. *Ultrasound Med. Biol.* **44**, 2540–2547 (2018).

142. Nightingale, K., Soo, M. S., Nightingale, R. & Trahey, G. Acoustic radiation force impulse imaging: in vivo demonstration of clinical feasibility. *Ultrasound Med. Biol.* **28**, 227–235 (2002).

143. Brandenburg, J. E. *et al.* Ultrasound Elastography: The New Frontier in Direct Measurement of Muscle Stiffness. *Arch. Phys. Med. Rehabil.* **95**, 2207–2219 (2014).

144. Hossain, M. M., Nichols, T., Merricks, E. & Gallippi, C. Viscoelastic response (VisR)-derived relative elasticity and relative viscosity reflect true elasticity and viscosity, in silico. in *2017 IEEE International Ultrasonics Symposium (IUS)* 1–4 (2017). doi:10.1109/ULTSYM.2017.8092884.

145. Eby, S. F. *et al.* Validation of shear wave elastography in skeletal muscle. *J. Biomech.* **46**, 2381–2387 (2013).

146. Bamber, J. *et al.* EFSUMB guidelines and recommendations on the clinical use of ultrasound elastography. Part 1: Basic principles and technology. *Ultraschall Med. Stuttg. Ger. 1980* **34**, 169–184 (2013).

147. Kronlage, C. *et al.* Muscle Ultrasound Shear Wave Elastography as a Non-Invasive Biomarker in Myotonia. *Diagnostics* **11**, 163 (2021).

148. Gennisson, J.-L., Deffieux, T., Fink, M. & Tanter, M. Ultrasound elastography: principles and techniques. *Diagn. Interv. Imaging* **94**, 487–495 (2013).

149. Barnes, S. L. & Simon, N. G. Clinical and research applications of neuromuscular ultrasound in amyotrophic lateral sclerosis. *Degener. Neurol. Neuromuscul. Dis.* **9**, 89–102 (2019).

150. Ryu, J. & Jeong, W. K. Current status of musculoskeletal application of shear wave elastography. *Ultrasonography* **36**, 185–197 (2017).

151. Stecco, A., Pirri, C., De Caro, R. & Raghavan, P. Stiffness and echogenicity: Development of a stiffness-echogenicity matrix for clinical problem solving. *Eur. J. Transl. Myol.* **29**, (2019).

152. Jerban, S., Barrère, V., Andre, M., Chang, E. Y. & Shah, S. B. Quantitative Ultrasound Techniques Used for Peripheral Nerve Assessment. *Diagnostics* **13**, 956 (2023).

153. Boom, J. & Visser, L. H. Quantitative assessment of nerve echogenicity: Comparison of methods for evaluating nerve echogenicity in ulnar neuropathy at the elbow. *Clin. Neurophysiol.* **123**, 1446–1453 (2012).

154. Tagliafico, A., Tagliafico, G. & Martinoli, C. Nerve Density: A New Parameter to Evaluate Peripheral Nerve Pathology on Ultrasound. Preliminary Study. *Ultrasound Med. Biol.* **36**, 1588–1593 (2010).

155. Watanabe, T. *et al.* Sonographic Evaluation of the Peripheral Nerve in Diabetic Patients The Relationship Between Nerve Conduction Studies, Echo Intensity, and Cross-sectional Area. *J. Ultrasound Med.* **29**, 697–708 (2010).

156. Beekman, R., Visser, L. H. & Verhagen, W. I. Ultrasonography in ulnar neuropathy at the elbow: a critical review. *Muscle Nerve* **43**, 627–635 (2011).

157. Tagliafico, A., Tagliafico, G. & Martinoli, C. Quantitative assessment of nerve echogenicity: A promising research tool? *Clin. Neurophysiol.* **124**, 209 (2013).

158. Downs, M. E. *et al.* Non-invasive peripheral nerve stimulation via focused ultrasound in vivo. *Phys. Med. Biol.* **63**, 035011 (2018).

159. Izzetti, R. *et al.* Ultra-High Frequency Ultrasound, A Promising Diagnostic Technique: Review of the Literature and Single-Center Experience. *Can. Assoc. Radiol. J.* **72**, 418–431 (2021).

160. Foster, F. S. *et al.* Principles and applications of ultrasound backscatter microscopy. *IEEE Trans. Ultrason. Ferroelectr. Freq. Control* **40**, 608–617 (1993).

161. Artur Bezugly. High frequency ultrasound study of skin tumors in dermatological and aesthetic practice. *Med. Ultrason.* **17**, (2015).

162. Shook, S. ULTRASOUND OF PERIPHERAL NERVE AND MUSCLE. in *2013 Conference for the American Society of Neuroimaging* (2013).

163. Cosgrove, D. O. Ultrasound and Contrast Ultrasound. in *Focal Liver Lesions: Detection, Characterization, Ablation* (eds. Lencioni, R., Cioni, D. & Bartolozzi, C.) 3–16 (Springer, 2005). doi:10.1007/3-540-26354-3_1.

164. Byra, M. *et al.* Quantitative Ultrasound and B-Mode Image Texture Features Correlate with Collagen and Myelin Content in Human Ulnar Nerve Fascicles. *Ultrasound Med. Biol.* **45**, 1830–1840 (2019).

165. Jakubovic, R. *et al.* High-Frequency Micro-Ultrasound Imaging and Optical Topographic Imaging for Spinal Surgery: Initial Experiences. *Ultrasound Med. Biol.* **44**, 2379–2387 (2018).

166. Viviano, S. L., Chandler, L. K. & Keith, J. D. Ultrahigh Frequency Ultrasound Imaging of the Hand: A New Diagnostic Tool for Hand Surgery. *HAND* **13**, 720–725 (2018).

167. Paluch, L. *et al.* Shear-wave elastography: a new potential method to diagnose ulnar neuropathy at the elbow. *Eur. Radiol.* **28**, 4932–4939 (2018).

168. He, Y., Xiang, X., Zhu, B.-H. & Qiu, L. Shear wave elastography evaluation of the median and tibial nerve in diabetic peripheral neuropathy. *Quant. Imaging Med. Surg.* **9**, 27382–27282 (2019).

169. Dikici, A. S. *et al.* Evaluation of the Tibial Nerve with Shear-Wave Elastography: *Musculoskelet. IMAGING* **282**, 8 (2017).

170. Ishibashi, F. *et al.* Elasticity of the tibial nerve assessed by sonoelastography was reduced before the development of neuropathy and further deterioration associated with the severity of neuropathy in patients with type 2 diabetes. *J. Diabetes Investig.* **7**, 404–412 (2016).

171. Aslan, M. *et al.* Assessment of Peripheral Nerves With Shear Wave Elastography in Type 1 Diabetic Adolescents Without Diabetic Peripheral Neuropathy. *J. Ultrasound Med.* **38**, 1583–1596 (2019).

172. Wei, M. & Ye, X. Feasibility of Point Shear Wave Elastography for Evaluating Diabetic Peripheral Neuropathy. *J. Ultrasound Med.* **39**, 1135–1141 (2020).

173. Tang, X. *et al.* Preliminary study on the influencing factors of shear wave elastography for peripheral nerves in healthy population. *Sci. Rep.* **11**, 5582 (2021).

174. Bedewi, M. A. *et al.* Shear wave elastography of the tibial nerve in healthy subjects. *Medicine (Baltimore)* **100**, e23999 (2021).

175. Zhu, B. *et al.* Evaluation of the healthy median nerve elasticity Feasibility and reliability of shear wave elastography. *Medicine (Baltimore)* **97**, (2018).

176. Wee, T. C. & Simon, N. G. Ultrasound elastography for the evaluation of peripheral nerves: A systematic review. *Muscle Nerve* **60**, 501–512 (2019).

177. Schrier, V. J. M. M. *et al.* Shear wave elastography of the median nerve: A mechanical study. *Muscle Nerve* **61**, 826–833 (2020).

178. Rugel, C., Franz, C. & Lee, S. Influence of limb position on assessment of nerve mechanical properties by using shear wave ultrasound elastography. *MUSCLE NERVE* **61**, 616–622 (2020).

179. Moon, J. H., Hwang, J.-Y., Park, J. S., Koh, S. H. & Park, S.-Y. Impact of region of interest (ROI) size on the diagnostic performance of shear wave elastography in differentiating solid breast lesions. *Acta Radiol.* **59**, 657–663 (2018).

180. Mulabecirovic, A., Vesterhus, M., Gilja, O. H. & Havre, R. F. In Vitro Comparison of Five Different Elastography Systems for Clinical Applications, Using Strain and Shear Wave Technology. *Ultrasound Med. Biol.* **42**, 2572–2588 (2016).

181. Dillman, J. R. *et al.* Superficial ultrasound shear wave speed measurements in soft and hard elasticity phantoms: repeatability and reproducibility using two ultrasound systems. *Pediatr. Radiol.* **45**, 376–385 (2015).

182. Shin, H. J., Kim, M.-J., Kim, H. Y., Roh, Y. H. & Lee, M.-J. Comparison of shear wave velocities on ultrasound elastography between different machines, transducers, and acquisition depths: a phantom study. *Eur. Radiol.* **26**, 3361–3367 (2016).

183. Greening, J. & Dilley, A. Posture-induced changes in peripheral nerve stiffness measured by ultrasound shear-wave elastography: Nerve Shear-wave Elastography. *MUSCLE NERVE* **55**, 213–222 (2017).

184. Zakrzewski, J., Zakrzewska, K., Pluta, K., Nowak, O. & Miłoszewska-Paluch, A. Ultrasound elastography in the evaluation of peripheral neuropathies: a systematic review of the literature. *Pol. J. Radiol.* **84**, 581–591 (2019).

185. Nam, K., Peterson, S. M., Wessner, C. E., Machado, P. & Forsberg, F. Diagnosis of Carpal Tunnel Syndrome using Shear Wave Elastography and High-frequency Ultrasound Imaging. *Acad. Radiol.* **28**, e278–e287 (2021).

186. Moran, L. *et al.* Carpal Tunnel Syndrome: Diagnostic Usefulness of Ultrasound Measurement of the Median Nerve Area and Quantitative Elastographic Measurement of the Median Nerve Stiffness. *J. Ultrasound Med.* **39**, 331–339 (2020).

187. Miyamoto, H. *et al.* Carpal Tunnel Syndrome: Diagnosis by Means of Median Nerve Elasticity—Improved Diagnostic Accuracy of US with Sonoelastography. *Radiology* **270**, 481–486 (2014).

188. Mohammadi, A., Ghasemi-Rad, M., Mladkova-Suchy, N. & Ansari, S. Correlation between the severity of carpal tunnel syndrome and color Doppler sonography findings. *AJR Am. J. Roentgenol.* **198**, W181-184 (2012).

189. Wee, T. C. & Simon, N. G. Shearwave Elastography in the Differentiation of Carpal Tunnel Syndrome Severity. *PM R* **12**, 1134–1139 (2020).

190. Ibrahim, H. R. Diagnostic value of median nerve shear wave ultrasound elastography in diagnosis and differentiation of carpal tunnel syndrome severity. *Egypt. J. Radiol. Nucl. Med.* **52**, 187 (2021).

191. Chen, J. *et al.* Value of superb microvascular imaging ultrasonography in the diagnosis of carpal tunnel syndrome: Compared with color Doppler and power Doppler. *Medicine (Baltimore)* **96**, e6862 (2017).

192. Paluch, Ł., Pietruski, P., Walecki, J. & Noszczyk, B. H. Wrist to forearm ratio as a median nerve shear wave elastography test in carpal tunnel syndrome diagnosis. *J. Plast. Reconstr. Aesthet. Surg.* **71**, 1146–1152 (2018).

193. Wang, T., Qi, H., Chen, C. & Teng, J. Study on the Crush Injury Model of the Sciatic Nerve in Rabbits by ConventionalUltrasound and Elastography. *Curr. Med. Imaging Former. Curr. Med. Imaging Rev.* **19**, 764–769 (2023).

194. Zhu, Y. *et al.* Evaluation of the Crushed Sciatic Nerve and Denervated Muscle with Multimodality Ultrasound Techniques: An Animal Study. *Ultrasound Med. Biol.* **46**, 377–392 (2020).

195. Kesikburun, S., Adigüzel, E., Kesikburun, B. & Yaşar, E. Sonoelastographic Assessment of the Median Nerve in the Longitudinal Plane for Carpal Tunnel Syndrome. *PM&R* **8**, 183–185 (2016).

196. Wang, Y., Tang, P., Zhang, L., Guo, Y. & Wan, W. Quantitative evaluation of the peripheral nerve blood perfusion with high frequency contrast-enhanced ultrasound. *Acad. Radiol.* **17**, 1492–1497 (2010).

197. Kele, H. Ultrasonography of the peripheral nervous system. *Perspect. Med.* **1**, 417–421 (2012).

198. Suk, J. I., Walker, F. O. & Cartwright, M. S. Ultrasound of Peripheral Nerves. *Curr. Neurol. Neurosci. Rep.* **13**, 328 (2013).

199. Tegtmeyer, K., Abboud, S. F., Omar, I. M., Grant, T. & Deshmukh, S. Musculoskeletal Ultrasound of Rheumatologic Conditions. *Adv. Clin. Radiol.* **3**, 169–182 (2021).

200. Wong, S. M. *et al.* Carpal Tunnel Syndrome: Diagnostic Usefulness of Sonography. *Radiology* **232**, 93–99 (2004).

201. Mallouhi, A. *et al.* Predictors of carpal tunnel syndrome: accuracy of gray-scale and color Doppler sonography. *AJR Am. J. Roentgenol.* **186**, 1240–1245 (2006).

202. Réaux-Le-Goazigo, A. *et al.* Ultrasound localization microscopy and functional ultrasound imaging reveal atypical features of the trigeminal ganglion vasculature. *Commun. Biol.* **5**, 330 (2022).

203. In Vitro Comparison of Five Different Elastography Systems for Clinical Applications, Using Strain and Shear Wave Technology - PubMed. https://pubmed.ncbi.nlm.nih.gov/27570209/.

204. Beard, P. Biomedical photoacoustic imaging. *Interface Focus* **1**, 602–631 (2011).

205. Ntziachristos, V. & Razansky, D. Molecular Imaging by Means of Multispectral Optoacoustic Tomography (MSOT). *Chem. Rev.* **110**, 2783–2794 (2010).

206. Bodea, S.-V. & Westmeyer, G. G. Photoacoustic Neuroimaging - Perspectives on a Maturing Imaging Technique and its Applications in Neuroscience. *Front. Neurosci.* **15**, (2021).

207. Taruttis, A. & Ntziachristos, V. Advances in real-time multispectral optoacoustic imaging and its applications. *Nat. Photonics* **9**, 219–227 (2015).

208. Omar, M., Soliman, D., Gateau, J. & Ntziachristos, V. Ultrawideband reflection-mode optoacoustic mesoscopy. *Opt. Lett.* **39**, 3911–3914 (2014).

209. Chaigne, T., Arnal, B., Vilov, S., Bossy, E. & Katz, O. Super-resolution photoacoustic imaging via flow-induced absorption fluctuations. *Optica* **4**, 1397–1404 (2017).

210. Schwarz, M. *et al.* Optoacoustic Dermoscopy of the Human Skin: Tuning Excitation Energy for Optimal Detection Bandwidth With Fast and Deep Imaging in vivo. *IEEE Trans. Med. Imaging* **36**, 1287–1296 (2017).

211. Soliman, D., Tserevelakis, G. J., Omar, M. & Ntziachristos, V. Combining microscopy with mesoscopy using optical and optoacoustic label-free modes. *Sci. Rep.* **5**, 12902 (2015).

212. Jeon, S., Kim, J., Lee, D., Baik, J. W. & Kim, C. Review on practical photoacoustic microscopy. *Photoacoustics* **15**, 100141 (2019).

213. Fan, Q. *et al.* Transferring Biomarker into Molecular Probe: Melanin Nanoparticle as a Naturally Active Platform for Multimodality Imaging. *J. Am. Chem. Soc.* **136**, 15185–15194 (2014).

214. Guggenheim, J. A. *et al.* Photoacoustic imaging of human lymph nodes with endogenous lipid and hemoglobin contrast. *J. Biomed. Opt.* **20**, 1 (2015).

215. Graham, M. T., von Guionneau, N., Tuffaha, S. & Lediju Bell, M. A. Design and optimization of simulated light delivery systems for photoacoustic assessment of peripheral nerve injury. in *Photons Plus Ultrasound: Imaging and Sensing 2022* (eds. Oraevsky, A. A. & Wang, L. V.) 169 (SPIE, 2022). doi:10.1117/12.2610511.

216. Ishihara, M. *et al.* Performance validation of improved photoacoustic / ultrasound superposed imaging system for evaluation of diabetic neuropathy. in *Photons Plus Ultrasound: Imaging and Sensing 2019* vol. 10878 433–440 (SPIE, 2019).

217. Mari, J. M., West, S., Beard, P. C. & Desjardins, A. E. Multispectral photoacoustic imaging of nerves with a clinical ultrasound system. in *Photons Plus Ultrasound: Imaging and Sensing 2014* vol. 8943 148–154 (SPIE, 2014).

218. Mari, J. M., Xia, W., West, S. J. & Desjardins, A. E. Interventional multispectral photoacoustic imaging with a clinical ultrasound probe for discriminating nerves and tendons: an ex vivo pilot study. *J. Biomed. Opt.* **20**, 110503 (2015).

219. Jüstel, D. *et al.* Spotlight on nerves: Portable multispectral optoacoustic imaging of peripheral nerve vascularization and morphology.

220. Li, R., Phillips, E., Wang, P., Goergen, C. J. & Cheng, J.-X. Label-free in vivo imaging of peripheral nerve by multispectral photoacoustic tomography. *J. Biophotonics* **9**, 124–128 (2016).

221. Matthews, T. P., Zhang, C., Yao, D.-K., Maslov, K. I. & Wang, L. V. Label-free photoacoustic microscopy of peripheral nerves. *J. Biomed. Opt.* **19**, 1 (2014).

222. Bell, A. G. Upon the production of sound by radiant energy. *Am. J. Sci.* **s3-21**, 463–490 (1881).

223. Steinberg, I. *et al.* Photoacoustic clinical imaging. *Photoacoustics* **14**, 77–98 (2019).

224. Vu, T., Razansky, D. & Yao, J. Listening to tissues with new light: recent technological advances in photoacoustic imaging. *J. Opt.* **21**, 103001 (2019).

225. Du, J., Yang, S., Qiao, Y., Lu, H. & Dong, H. Recent progress in near-infrared photoacoustic imaging. *Biosens. Bioelectron.* **191**, 113478 (2021).

226. Dong, B., Yao, J. & Deán-Ben, X. L. Editorial: Advances in Photoacoustic Neuroimaging. *Front. Neurosci.* (2022) doi:10.3389/fnins.2022.859515.

227. A review of clinical photoacoustic imaging: Current and future trends. *Photoacoustics* **16**, 100144 (2019).

228. Ovsepian, S. V., Olefir, I., Westmeyer, G., Razansky, D. & Ntziachristos, V. Pushing the Boundaries of Neuroimaging with Optoacoustics. *Neuron* **96**, 966–988 (2017).

229. Das, D., Sharma, A., Rajendran, P. & Pramanik, M. Another decade of photoacoustic imaging. *Phys. Med. Biol.* **66**, 05TR01 (2021).

230. Lengenfelder, B. *et al.* Remote photoacoustic sensing using speckle-analysis. *Sci. Rep.* **9**, 1057 (2019).

231. Wang, L. V. & Hu, S. Photoacoustic Tomography: In Vivo Imaging from Organelles to Organs. *Science* **335**, 1458–1462 (2012).

232. Wu, W., Wang, P., Cheng, J.-X. & Xu, X.-M. Assessment of White Matter Loss Using Bond-Selective Photoacoustic Imaging in a Rat Model of Contusive Spinal Cord Injury. *J. Neurotrauma* **31**, 1998–2002 (2014).

233. Luzhansky, I. D., Sudlow, L. C., Brogan, D. M., Wood, M. D. & Berezin, M. Y. Imaging in the repair of peripheral nerve injury. *Nanomed.* **14**, 2659–2677 (2019).

234. Chen, K.-T., Wei, K.-C. & Liu, H.-L. Theranostic Strategy of Focused Ultrasound Induced Blood-Brain Barrier Opening for CNS Disease Treatment. *Front. Pharmacol.* **10**, 86 (2019).

235. Zhu, Y. *et al.* Light Emitting Diodes based Photoacoustic Imaging and Potential Clinical Applications. *Sci. Rep.* **8**, 9885 (2018).

236. Lin, L. & Wang, L. V. Photoacoustic Imaging. in (eds. Wei, X. & Gu, B.) 147–175 (Springer Singapore, 2021).

237. Plumb, A. A., Huynh, N. T., Guggenheim, J., Zhang, E. & Beard, P. Rapid volumetric photoacoustic tomographic imaging with a Fabry-Perot ultrasound sensor depicts peripheral arteries and microvascular vasomotor responses to thermal stimuli. *Eur. Radiol.* **28**, 1037–1045 (2018).

238. Wissmeyer, G., Pleitez, M. A., Rosenthal, A. & Ntziachristos, V. Looking at sound: optoacoustics with all-optical ultrasound detection. *Light Sci. Appl.* **7**, 53 (2018).

239. Rosenthal, A., Ntziachristos, V. & Razansky, D. Acoustic Inversion in Optoacoustic Tomography: A Review. *Curr. Med. Imaging Rev.* **9**, 318–336 (2013).

240. Gottschalk, S. *et al.* Rapid volumetric optoacoustic imaging of neural dynamics across the mouse brain. *Nat. Biomed. Eng.* **3**, 392–401 (2019).

241. Shen, C. *et al.* An introduction to deep learning in medical physics: advantages, potential, and challenges. *Phys. Med. Biol.* **65**, 05TR01 (2020).

242. Pradhan, P., Guo, S., Ryabchykov, O., Popp, J. & Bocklitz, T. W. Deep learning a boon for biophotonics? *J. Biophotonics* **13**, e201960186 (2020).

243. Hysi, E., Moore, M. J., Strohm, E. M. & Kolios, M. C. A tutorial in photoacoustic microscopy and tomography signal processing methods. *J. Appl. Phys.* **129**, 141102 (2021).

244. Luís Dean-Ben, X. & Razansky, D. Localization optoacoustic tomography. *Light Sci. Appl.* **7**, 18004–18004 (2018).

245. Yu, Z. *et al.* Wavefront shaping: A versatile tool to conquer multiple scattering in multidisciplinary fields. *The Innovation* **3**, 100292 (2022).

246. Lai, P., Wang, L., Tay, J. W. & Wang, L. V. Photoacoustically guided wavefront shaping for enhanced optical focusing in scattering media. *Nat. Photonics* **9**, 126–132 (2015).

247. Dertinger, T., Colyer, R., Iyer, G., Weiss, S. & Enderlein, J. Fast, background-free, 3D super-resolution optical fluctuation imaging (SOFI). *Proc. Natl. Acad. Sci.* **106**, 22287–22292 (2009).

248. Conkey, D. B. *et al.* Super-resolution photoacoustic imaging through a scattering wall. *Nat. Commun.* **6**, 7902 (2015).

249. Behera, D., Jacobs, K. E., Behera, S., Rosenberg, J. & Biswal, S. 18 F-FDG PET/MRI Can Be Used to Identify Injured Peripheral Nerves in a Model of Neuropathic Pain. *J. Nucl. Med.* **52**, 1308–1312 (2011).

250. Rangavajla, G., Mokarram, N., Masoodzadehgan, N., Pai, S. B. & Bellamkonda, R. V. Noninvasive Imaging of Peripheral Nerves. *Cells Tissues Organs* **200**, 69–77 (2015).

251. Nam, J. W., Lee, M. J. & Kim, H. J. Diagnostic Efficacy of 18F-FDG PET/MRI in Peripheral Nerve Injury Models. *Neurochem. Res.* **44**, 2092–2102 (2019).

252. Stoll, G., Israel, I., Deiss, A. & Samnik, S. Macrophage imaging in experimental nerve injury by 68GA-dotatate: A combined autoradiography/pet study - Record details - Embase. in *Journal of the Peripheral Nervous System* vol. 21 214 (2016).

253. Ewertsen, C., Săftoiu, A., Gruionu, L. G., Karstrup, S. & Nielsen, M. B. Real-Time Image Fusion Involving Diagnostic Ultrasound. *Am. J. Roentgenol.* **200**, W249–W255 (2013).

254. Wein, W. *et al.* Global Registration of Ultrasound to MRI Using the LC2 Metric for Enabling Neurosurgical Guidance. in *Medical Image Computing and Computer-Assisted Intervention – MICCAI 2013* (eds. Mori, K., Sakuma, I., Sato, Y., Barillot, C. & Navab, N.) 34–41 (Springer, 2013). doi:10.1007/978-3-642-40811-3_5.

255. Chopra, S. S. *et al.* Development and validation of a three dimensional ultrasound based navigation system for tumor resection. *Eur. J. Surg. Oncol. EJSO* **34**, 456–461 (2008).

256. Heinrich, M. P. Intra-operative Ultrasound to MRI Fusion with a Public Multimodal Discrete Registration Tool. in *Simulation, Image Processing, and Ultrasound Systems for Assisted Diagnosis and Navigation* (eds. Stoyanov, D. et al.) 159–164 (Springer International Publishing, 2018). doi:10.1007/978-3-030-01045-4_19.

257. Attia, A. B. E. *et al.* Multispectral optoacoustic and MRI coregistration for molecular imaging of orthotopic model of human glioblastoma. *J. Biophotonics* **9**, 701–708 (2016).

258. Lee, C., Choi, W., Kim, J. & Kim, C. Three-dimensional clinical handheld photoacoustic/ultrasound scanner. *Photoacoustics* **18**, 100173 (2020).

259. Bilgen, M. *et al.* Microneurography of human median nerve. *J. Magn. Reson. Imaging JMRI* **21**, 826–830 (2005).

260. Yoon, D., Biswal, S., Rutt, B., Lutz, A. & Hargreaves, B. Feasibility of 7T MRI for Imaging Fascicular Structures of Peripheral Nerves. *Muscle Nerve* **57**, 494–498 (2018).

261. Felisaz, P. F. *et al.* In Vivo MR Microneurography of the Tibial and Common Peroneal Nerves. *Radiol. Res. Pract.* **2014**, 1–6 (2014).

262. Riegler, G. *et al.* High-Resolution Axonal Bundle (Fascicle) Assessment and Triple-Echo Steady-State T2 Mapping of the Median Nerve at 7 T: Preliminary Experience. *Invest. Radiol.* **51**, 529–535 (2016).

263. Zochowski, K. C. *et al.* Improvement of peripheral nerve visualization using a deep learning-based MR reconstruction algorithm. *Magn. Reson. Imaging* **85**, 186–192 (2022).

264. Felisaz, P. F. *et al.* Nerve Fascicles and Epineurium Volume Segmentation of Peripheral Nerve Using Magnetic Resonance Micro-neurography. *Acad. Radiol.* **23**, 1000–1007 (2016).

265. Evans, M. C. *et al.* Magnetic Resonance Imaging as a Biomarker in Diabetic and HIV-Associated Peripheral Neuropathy: A Systematic Review-Based Narrative. *Front. Neurosci.* **15**, 727311 (2021).

266. Sodickson, D. K., Griswold, M. A., Jakob, P. M., Edelman, R. R. & Manning, W. J. Signal-to-noise ratio and signal-to-noise efficiency in SMASH imaging. *Magn. Reson. Med.* **41**, 1009–1022 (1999).

267. Lustig, M., Donoho, D. & Pauly, J. M. Sparse MRI: The application of compressed sensing for rapid MR imaging. *Magn. Reson. Med.* **58**, 1182–1195 (2007).

268. Felisaz, P. *et al.* MR microneurography and quantitative T2 and DP measurements of the distal tibial nerve in CIDP. *J. Neurol. Sci.* **400**, 15–20 (2019).

269. Shung, K. K. High Frequency Ultrasonic Imaging. *J. Med. Ultrasound* **17**, 25–30 (2009).

270. Pavlin, C. J., Harasiewicz, K., Sherar, M. D. & Foster, F. S. Clinical Use of Ultrasound Biomicroscopy. *Ophthalmology* **98**, 287–295 (1991).

271. Foster, F. S., Pavlin, C. J., Harasiewicz, K. A., Christopher, D. A. & Turnbull, D. H. Advances in ultrasound biomicroscopy. *Ultrasound Med. Biol.* **26**, 1–27 (2000).

272. Henry, F. P. *et al.* In vivo optical microscopy of peripheral nerve myelination with polarization sensitive-optical coherence tomography. *J. Biomed. Opt.* **20**, 046002 (2015).

273. Nam, A. *et al.* Wide-Field Functional Microscopy of Peripheral Nerve Injury and Regeneration. *Sci. Rep.* **8**, (2018).

274. Bélanger, E. *et al.* Quantitative myelin imaging with coherent anti-Stokes Raman scattering microscopy: alleviating the excitation polarization dependence with circularly polarized laser beams. *Opt. Express* **17**, 18419 (2009).

275. Jung, Y. *et al.* Comprehensive Evaluation of Peripheral Nerve Regeneration in the Acute Healing Phase Using Tissue Clearing and Optical Microscopy in a Rodent Model. *PLoS ONE* **9**, e94054 (2014).

276. Fujimoto, J. G., Pitris, C., Boppart, S. A. & Brezinski, M. E. Optical Coherence Tomography: An Emerging Technology for Biomedical Imaging and Optical Biopsy. *Neoplasia N. Y. N* **2**, 9–25 (2000).

277. Cotero, V. E. *et al.* Improved Intraoperative Visualization of Nerves through a Myelin-Binding Fluorophore and Dual-Mode Laparoscopic Imaging. *PLOS ONE* **10**, e0130276 (2015).

278. Walsh, E. M. *et al.* Fluorescence Imaging of Nerves During Surgery. *Ann. Surg.* **270**, 69–76 (2019).

279. Gibbs-Strauss, S. L. *et al.* Nerve-Highlighting Fluorescent Contrast Agents for Image-Guided Surgery. *Mol. Imaging* **10**, 7290.2010.00026 (2011).

280. Yan, Y. Evaluation of peripheral nerve regeneration via in vivo serial transcutaneous imaging using transgenic Thy1-YFP mice. *Exp. Neurol.* 8 (2011).

281. Bremer, J., Skinner, J. & Granato, M. A small molecule screen identifies in vivo modulators of peripheral nerve regeneration in zebrafish. *PLOS ONE* **12**, e0178854 (2017).

282. Placheta, E. *et al.* Macroscopic In Vivo Imaging of Facial Nerve Regeneration in *Thy1 - GFP* Rats. *JAMA Facial Plast. Surg.* **17**, 8–15 (2015).

283. MicroCT optimisation for imaging fascicular anatomy in peripheral nerves. *J. Neurosci. Methods* **338**, 108652 (2020).

284. Heimel, P. *et al.* Iodine-Enhanced Micro-CT Imaging of Soft Tissue on the Example of Peripheral Nerve Regeneration. *Contrast Media Mol. Imaging* **2019**, 7483745–15 (2019).

285. Morisaki, S. *et al.* Application of Raman spectroscopy for visualizing biochemical changes during peripheral nerve injury *in vitro* and *in vivo*. *J. Biomed. Opt.* **18**, 116011 (2013).

286. Kumamoto, Y., Harada, Y., Tanaka, H. & Takamatsu, T. Rapid and accurate peripheral nerve imaging by multipoint Raman spectroscopy. *Sci. Rep.* **7**, 845 (2017).

287. Boon, A. J. Neuromuscular Ultrasound in the EMG Laboratory. in *Clinical Neurophysiology* (eds. Rubin, D. I. & Rubin, D. I.) 0 (Oxford University Press, 2021). doi:10.1093/med/9780190067854.003.0037.

288. Preston, D. C. & Shapiro, B. E. *Electromyography and neuromuscular disorders e-book: clinical-electrophysiologic-ultrasound correlations*. (Elsevier Health Sciences, 2020).

289. Strommen, J. A., Skinner, S. & Crum, B. A. Neurophysiology during peripheral nerve surgery. in *Handbook of Clinical Neurology* vol. 186 295–318 (Elsevier, 2022).

290. Haldeman, C. L., Baggott, C. D. & Hanna, A. S. Intraoperative ultrasound-assisted peripheral nerve surgery. *Neurosurg. Focus* **39**, E4 (2015).

291. Koenig, R. W. *et al.* Intraoperative high-resolution ultrasound: a new technique in the management of peripheral nerve disorders: Clinical article. *J. Neurosurg.* **114**, 514–521 (2011).

292. Burks, S. S., Cajigas, I., Jose, J. & Levi, A. D. Intraoperative Imaging in Traumatic Peripheral Nerve Lesions: Correlating Histologic Cross-Sections with High-Resolution Ultrasound. *Oper. Neurosurg.* **13**, 196–203 (2017).

293. Chiou, H.-J., Chou, Y.-H., Chiou, S.-Y., Liu, J.-B. & Chang, C.-Y. Peripheral nerve lesions: role of high-resolution US. *Radiographics* **23**, e15–e15 (2003).

294. Gofeld, M., Bristow, S. J., Chiu, S. & Kliot, M. Preoperative ultrasound-guided mapping of peripheral nerves: Laboratory investigation. *J. Neurosurg.* **119**, 709–713 (2013).

295. Boczar, D. *et al.* Intraoperative evaluation of cervical nerve root avulsion using ultra–high-frequency ultrasound system. *Case Rep. Plast. Surg. Hand Surg.* **6**, 43–46 (2019).

296. Forte, A. J., Boczar, D., Oliver, J. D., Sisti, A. & Clendenen, S. R. Ultra-high-frequency Ultrasound to Assess Nerve Fascicles in Median Nerve Traumatic Neuroma. *Cureus* **11**, e4871.

297. Hayashi, A. *et al.* Ultra High-frequency Ultrasonographic Imaging with 70 MHz Scanner for Visualization of the Lymphatic Vessels. *Plast. Reconstr. Surg. – Glob. Open* **7**, e2086 (2019).

298. Yeoh, S. *et al.* Incorporating Blood Flow in Nerve Injury and Regeneration Assessment. *Front. Surg.* **9**, 862478 (2022).

299. Ogata, K. & Naito, M. Blood flow of peripheral nerve effects of dissection stretching and compression. *J. Hand Surg. Br. Eur. Vol.* **11**, 10–14 (1986).

300. Artul, S., Nseir, W., Armaly, Z. & Soudack, M. Superb Microvascular Imaging: Added Value and Novel Applications. *J. Clin. Imaging Sci.* **7**, 45 (2017).

301. Járay, Á., Farkas, P. I., Semjén, D., Battyáni, I. & Botz, B. Additional value of microvascular flow imaging in the assessment of cystic and solid renal lesions. *Physiol. Int.* **110**, 52–63 (2023).

302. Höke, A., Sun, H. S., Gordon, T. & Zochodne, D. W. Do denervated peripheral nerve trunks become ischemic? The impact of chronic denervation on vasa nervorum. *Exp. Neurol.* **172**, 398–406 (2001).

303. Lee, C., Lee, D., Zhou, Q., Kim, J. & Kim, C. Real-time Near-infrared Virtual Intraoperative Surgical Photoacoustic Microscopy. *Photoacoustics* **3**, 100–106 (2015).

304. Abbasi, S. *et al.* All-optical Reflection-mode Microscopic Histology of Unstained Human Tissues. *Sci. Rep.* **9**, 13392 (2019).

305. Ecclestone, B. R. *et al.* Improving maximal safe brain tumor resection with photoacoustic remote sensing microscopy. *Sci. Rep.* **10**, 17211 (2020).

306. Ravagli, E. *et al.* Fascicle localisation within peripheral nerves through evoked activity recordings: A comparison between electrical impedance tomography and multi-electrode arrays. *J. Neurosci. Methods* 109140 (2021) doi:10.1016/j.jneumeth.2021.109140.

307. Ravagli, E. *et al.* Imaging fascicular organization of rat sciatic nerves with fast neural electrical impedance tomography. *Nat. Commun.* **11**, 6241 (2020).